Check for updates

MXene Electrocatalysts

How to cite:
International Edition: doi.org/10.1002/anie.202210828
German Edition: doi.org/10.1002/ange.202210828

Advancing MXene Electrocatalysts for Energy Conversion Reactions: Surface, Stoichiometry, and Stability

Constantine Tsounis, Priyank V. Kumar, Hassan Masood, Rutvij Pankaj Kulkarni, Gopalakrishnan Sai Gautam, Christoph R. Müller, Rose Amal, and Denis A. Kuznetso**

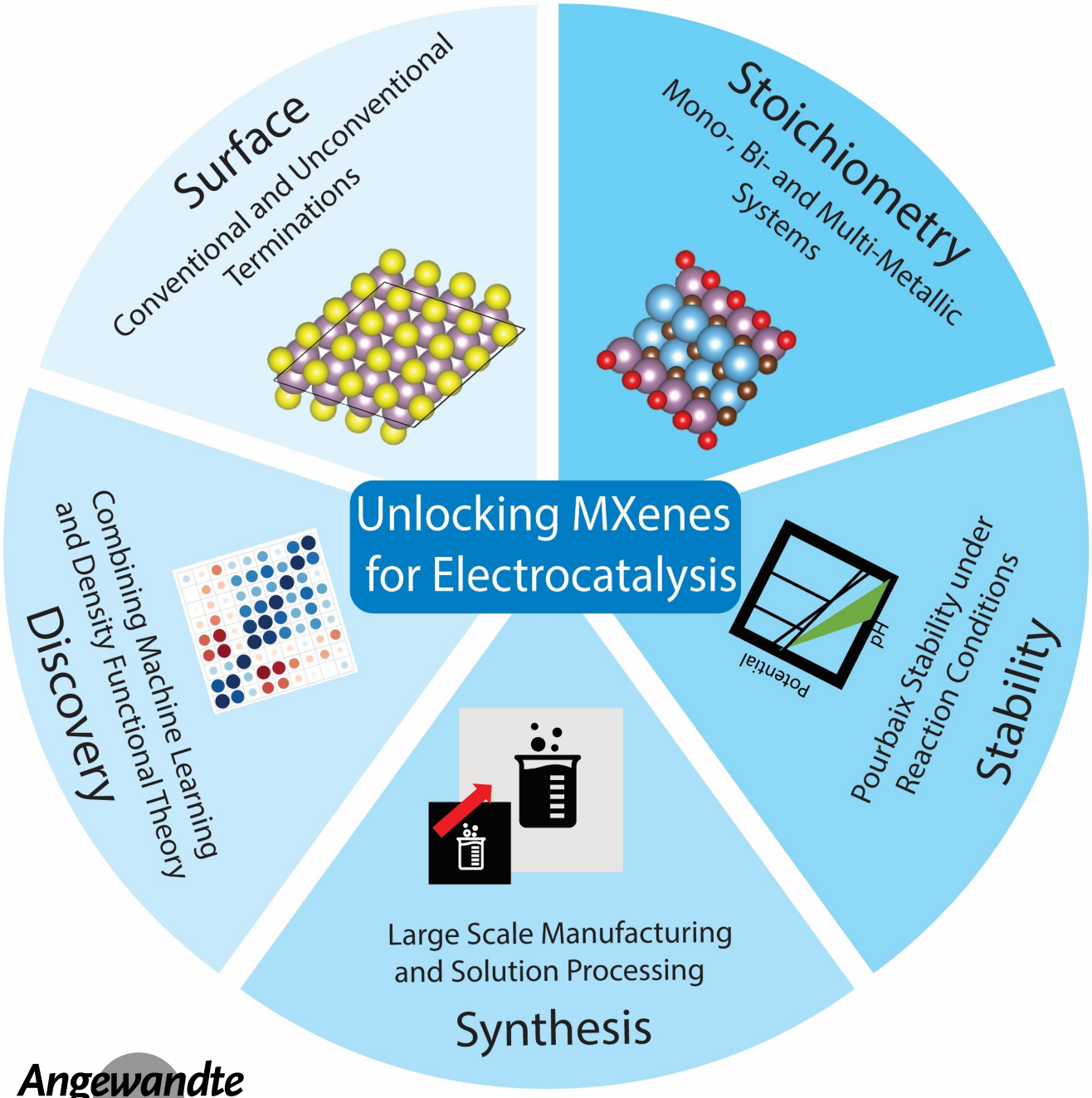

© 2022 The Authors. Angewandte Chemie International Edition published by Wiley-VCH GmbH

15213773, 0, Downloaded from https://onlinelibrary.wiley.com/doi/10.1002/anie.202210828 by National Medical Library The Director, Wiley Online Library on [01/12/2022]. See the Terms and Conditions (https://onlinelibrary.wiley.com/terms-and-conditions) on Wiley Online Library for rules of use; OA articles are governed by the applicable Creative Commons License

Abstract: MXenes, due to their tailorable chemistry and favourable physical properties, have great promise in electrocatalytic energy conversion reactions. To exploit fully their enormous potential, further advances specific to electrocatalysis revolving around their performance, stability, compositional discovery and synthesis are required. The most recent advances in these aspects are discussed in detail: surface functional and stoichiometric modifications which can improve performance, Pourbaix stability related to their electrocatalytic operating conditions, density functional theory and advances in machine learning for their discovery, and prospects in large scale synthesis and solution processing techniques to produce membrane electrode assemblies and integrated electrodes. This Review provides a perspective that is complemented by new density functional theory calculations which show how these recent advances in MXene material design are paving the way for effective electrocatalysts required for the transition to integrated renewable energy systems.

1. Introduction

Globally, sustainable energy systems are required to respond adequately to the rapidly changing climate induced through the substantial release of greenhouse gases.[1] To accomplish this, a framework relying on the use of renewable energy resources and sustainable energy carriers is required.[2] A key element of such a framework is electrochemical energy conversion reactions which produce sustainable chemicals and fuels such as hydrogen (through water splitting), ammonia (through dinitrogen or nitrate reduction), hydrogen peroxide (through oxygen reduction), and hydrocarbons and syngas (including acids, alcohols, alkanes and alkenes through CO_2 reduction) from renewable electricity.[3] These electrochemical energy conversion reactions allow for the sustainable production of fuels and chemical feedstocks supporting global decarbonization efforts and provide a means to store intermittent renewable electricity.

To unleash the potential of electrochemical energy conversion reactions, the development of highly efficient electrocatalytic materials is essential.[4–6] These materials are required to harness and convert renewable electricity into viable products at high rates, selectivity and stability. The performance of electrocatalysts depends on a range of chemical properties which are ultimately related to their electronic properties that in turn influence the intrinsic activity of the material, as well as their morphology which provides access to the catalytically active sites. Equally, the stability of the catalyst and its susceptibility to transformations and deactivation over time must be considered in their assessment. Furthermore, in order to maximize the application space of electrocatalysts, they must have specific manufacturing capabilities such that they can be synthesized and processed on large scales, while having the ability to be integrated on different electrode or membrane configurations according to specific electrolyzer cell and stack designs.[7]

MXenes, discovered in 2011 at Drexel University, are defined as two-dimensional (2D) transition metal carbides or nitrides, with the formula $M_{n+1}X_nT_x$, where M is an early transition metal (Mo, Ti, V, Nb, Hf, etc.), X is C and/or N, T_x represents the surface functional groups (O, OH, F, etc.) and $n=1$–4.[8] As different metals (and mixtures thereof) can be incorporated into the MXene structure, as well as considering its layered configuration and the presence of functional groups, there is effectively an unlimited number of MXene structures with variable band structures, providing a plethora of possibilities to tailor their chemical and physical properties, essential in the design of electrocatalysts.[9] Further desirable properties such as a metallic conductivity, high stability in a wide pH range in anaerobic conditions, flexible reduction–oxidation characteristics and high mechanical strength favour their use as electrocatalysts. Importantly, compared to other 2D materials such as MoS_2 (which, for example, demonstrates weak hydrogen adsorption on the basal plane), the basal planes of MXenes have been shown to be active for electrocatalytic redox reactions due to their specific terminating functional groups.[10,11] This negates the need to create complex architectures or to perform treatments to increase the exposure and density of active sites as often required for other 2D materials.[12] Based on these favourable physical and chemical properties, MXenes, when rationally designed and operated under judicious conditions (i.e. with a suitable stoichiometry, surface composition, choice of electrolyte and operating potential), have the potential to serve as promising electrocatalytic materials for energy conversion reactions. We note that MXenes also demonstrate promising tribological, magnetic, electronic, thermal and optical properties which allow for their application as lubricants, electro-

[*] C. Tsounis, Dr. P. V. Kumar, Dr. H. Masood, Prof. R. Amal
School of Chemical Engineering
The University of New South Wales
Kensington, NSW 2052 (Australia)
E-mail: c.tsounis@unsw.edu.au
C. Tsounis, Prof. C. R. Müller, Dr. D. A. Kuznetso
Department of Mechanical and Process Engineering
ETH Zurich
8092 Zurich (Switzerland)
E-mail: denisk@ethz.ch
R. P. Kulkarni, Prof. G. S. Gautam
Department of Materials Engineering
Indian Institute of Science
Bengaluru 560012 (India)

© 2022 The Authors. Angewandte Chemie International Edition published by Wiley-VCH GmbH. This is an open access article under the terms of the Creative Commons Attribution Non-Commercial NoDerivs License, which permits use and distribution in any medium, provided the original work is properly cited, the use is non-commercial and no modifications or adaptations are made.

15213773, 0, Downloaded from https://onlinelibrary.wiley.com/doi/10.1002/anie.202210828 by National Medical Library The Director, Wiley Online Library on [01/12/2022]. See the Terms and Conditions (https://onlinelibrary.wiley.com/terms-and-conditions) on Wiley Online Library for rules of use; OA articles are governed by the applicable Creative Commons License

Constantine Tsounis obtained his bachelor's degree in chemical engineering with honours at the University of New South Wales (UNSW) in 2018. He is currently undertaking a Ph.D. in the Particles and Catalysis Research group at the same institution. During his Ph.D., he was a visiting scholar at the department of mechanical and process engineering at ETH Zurich, and at the Commonwealth Scientific and Industrial Research Organisation (CSIRO). His research interests revolve around the fundamental development and application of photo- and electrocatalysts for various energy conversion reactions.

Priyank Vijaya Kumar is a Scientia Senior Lecturer in chemical engineering at UNSW Sydney, Australia. His research group is interested in understanding and designing nanomaterials using theory, computation and data-driven methods including density functional theory (DFT), time-dependent DFT (TDDFT), molecular dynamics and machine learning. The group focuses on applications such as photo-/electro-/thermocatalytic systems, batteries, functional polymers and water/gas separation membranes, and strives to collaborate with experimentalists in the relevant areas. Prior to UNSW, he pursued his Ph.D. in materials science and engineering at Massachusetts Institute of Technology, USA and carried out postdoctoral research at ETH Zurich, Switzerland.

Hassan Masood is a Data Scientist working with NSW eHealth. He received his Ph.D. in 2019 from School of Chemical Engineering at University of New South Wales, with computational fluid dynamics as the area of research. He worked with Particles and Catalysis Research Laboratory at the University of New South Wales on solving materials science problems via machine learning and data science approaches.

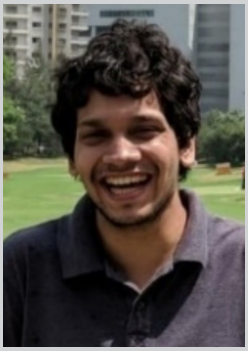

Rutvij Pankaj Kulkarni is a Project Associate with the SAI MATerials group at the Indian Institute of Science (IISc) in Bengaluru. In 2021, he graduated from the Mechanical Engineering bachelors program at the Birla Institute of Technology and Science, Pilani (Hyderabad Campus). His research at IISc aims to use machine learning with density functional theory calculations in solid electrolyte systems. He is keen on using modern computational methods in problems of science and engineering and he will be pursuing a masters in applied computational science at Imperial College London from October 2022.

Gopalakrishnan Sai Gautam is an Assistant Professor of Materials Engineering at Indian Institute of Science since 2020. He graduated with a Ph.D. in Materials Science and Engineering at Massachusetts Institute of Technology and followed that with a post-doctoral stint in Mechanical and Aerospace Engineering at Princeton University. His research interests are in the broad area of computational materials science, where he uses a combination of density functional theory calculations and machine learning tools for materials design in energy storage and energy harvesting applications.

Christoph Müller obtained a diploma in mechanical/process engineering from TU Munich in 2004 and a Ph.D. in chemical engineering from the University of Cambridge in 2008, under the supervision of Prof. John Dennis. In 2010, he became assistant professor at the department of mechanical and process engineering at ETH Zurich. Since 2018, he is full professor at the same institution. His research group is active in the development of CO_2 sorbents and catalysts as well as studying single- and multiphase granular flows.

Rose Amal is a Scientia Professor in the School of Chemical Engineering, UNSW Sydney and is the Director of the ARC Training Centre for the Global Hydrogen Economy. Her research focuses on designing nanomaterials for solar to chemical energy conversion applications and engineering systems for solar induced processes. She is a Fellow of the Australian Academy of Technological Sciences and Engineering (FTSE) and a Fellow of the Australian Academy of Science (FAA). She has received the nation's top civilian honour—the Companion of the Order of Australia—as part of the 2018 Queen's Birthday Honours for her eminent service to chemical engineering, was named 2019 NSW Scientist of the Year and was awarded the 2021 Chemeca Medal by the ANZFChE and the 2021 James Cook Medal by the Royal Society of NSW.

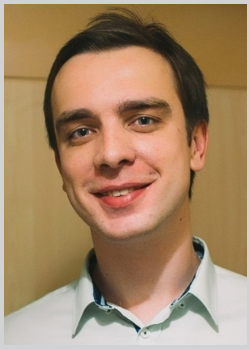

Denis Kuznetsov obtained his Ph.D. degree in Inorganic Chemistry from the Lomonosov Moscow State University in 2015 for his work on the development of synthetic approaches to molybdenum alkoxide complexes for N_2 reduction in the group of Dr. T. Bazhenova (Russian Academy of Sciences, Chernogolovka). He then moved to Massachusetts Institute of Technology to become a postdoctoral fellow (2017–2018) in the group of Prof. Y. Shao-Horn, switching to the area of electrocatalysis. Since 2018 he has been a postdoctoral research fellow at ETH Zurich with Prof. C. Müller, where his studies focus on unraveling fundamental structure–performance relationships in electrocatalysis to guide the design of materials for energy storage and conversion applications.

© 2022 The Authors. Angewandte Chemie International Edition published by Wiley-VCH GmbH

15213773, 0, Downloaded from https://onlinelibrary.wiley.com/doi/10.1002/anie.202210828 by National Medical Library The Director, Wiley Online Library on [01/12/2022]. See the Terms and Conditions (https://onlinelibrary.wiley.com/terms-and-conditions) on Wiley Online Library for rules of use; OA articles are governed by the applicable Creative Commons License

magnetic interference shields, sensors, supercapacitors, etc.[13]

Regarding their catalytic performance, despite the favourable properties that MXenes possess, there is only a limited number of reports in which these materials, rather than their derivatives, have shown satisfactory electrocatalytic performance in energy conversion reactions. So far, the works reporting on the use of MXenes (most commonly $Ti_3C_2T_x$, Ti_2CT_x and Mo_2CT_x) for energy conversion reactions indicate that appropriate modifications to their pristine structure must be undertaken to create favourable electrocatalytic active sites.[14–16] The intrinsic catalytic performance of MXenes can be altered through a range of approaches, primarily through manipulation of their surface properties (altering the conventional terminating groups and incorporation of non-native surface atoms) and bulk stoichiometry (through doping/substitution, defects, solid solution and ordered alloy formation) which subsequently leads to changes in reactivity.[17] While these advances in MXene synthesis are interesting from a fundamental point of view, so far, there is limited application on reactions beyond water splitting, e.g. dinitrogen and carbon dioxide reduction. Furthermore, recent advances in the development of MXenes to alter their surface and bulk properties, namely, the synthesis of high entropy MXenes with multiple M species,[18] and the rational tuning of surface terminations with unconventional functional groups,[19] have had no reported application in electrochemical energy conversion reactions. These recent advances give promise in advancing traditional modification approaches for MXenes which serve as electrocatalysts for a range of energy conversion reactions.

Further to this, the stability of MXenes under electrochemical conditions must be carefully considered. Particularly innate to oxygen electrocatalysis (such as oxygen evolution or oxygen reduction) where MXenes are prone to oxidation, composite catalyst configurations often involving one or two co-catalysts are used in conjunction with the MXene.[20] However, there is an ambiguity about the state of the MXene under in situ conditions due to the dynamic nature of MXenes, which are prone to structural changes and/or decomposition.[21,22] Questions on whether the original MXene or rather decomposition products of the MXene are the catalytically active material are often overlooked. Theoretical works demonstrate that the stability regions of some MXenes under an applied potential are limited, and that the surface terminations of MXenes change considerably with the pH of the media, which may alter their catalytic performance.[23–25] Hence further work is required to determine the stability of commonly used MXenes under typical electrochemical conditions (i.e. under potential and at low or high pH). These considerations have often been neglected in the recent literature and are pivotal to the advancement of high performing and stable MXenes used in energy conversion reactions.

This Review entails some of the most recent emerging findings and opportunities in MXene design, characterization, and applications which are beneficial for their performance in electrocatalytic energy conversion reactions. We discuss discoveries such as high entropy MXenes which present a new route to improving the location of MXenes on Sabatier volcano plots[26,27] and surface terminations which extend beyond the conventional O, OH, F and Cl groups which drastically alter surface reactivity. Regarding the stability of MXenes under electrochemical conditions, we discuss considerations that must be taken into account to determine the dynamic structure of MXenes under electrochemical conditions and provide new insights into the performance and stability of MXenes through a preliminary investigation using density functional theory (DFT) calculations and Pourbaix diagrams. In addition to this, we also give a perspective on the future of computational design of MXenes using machine learning and DFT, which considers the large combinatorial parameter space inherent to MXenes particularly when tuning MXene stoichiometry and surface chemistry. Finally, when considering industrial applications, we discuss relevant solution processing and manufacturing techniques which could allow for the handling and synthesis of MXenes on a larger scale.

It is of our view that if opportunities in these four areas, that is, performance (through surface and bulk stoichiometric modifications), stability, discovery and large-scale manufacturing can be addressed, MXenes can play a significant role as catalysts in the clean energy transition.

2. MXene Stoichiometry

Bulk stoichiometry directly influences the chemical properties of MXenes which in turn affect their electrochemical reactivity. Briefly, we outline some of the significant advances in MXene stoichiometry related to electrocatalysis, as displayed in Figure 1, before discussing in more detail the potential opportunities surrounding the further application of single atom-modified MXenes and the emerging area of high entropy MXenes related to electrocatalysis.

2.1. Monometallic MXenes

2.1.1. Common MXenes

Single-metal MXenes ($M_{n+1}X_nT_x$) are the most simple variation of MXene materials. They offer a well-defined yet tuneable platform for the discovery and investigation of MXenes for a range of energy conversion reactions. Regarding the hydrogen evolution reaction (HER), Seh et al. undertook a DFT screening to compare the theoretical performance of a range of single-metal MXenes after determining the most likely functional group configuration.[11] A range of MXenes with favourable HER theoretical overpotentials (<0.2 V) were identified, including Sc_2C and Mo_2C, of which Mo_2C had one of the lowest overpotentials of approximately 0.05 V. In the same work, corroborating their theoretical investigations, Mo_2C and Ti_2C were experimentally compared on the basis of their electrochemical performance, with Mo_2C outperforming Ti_2C. To improve the performance of the single-metal

© 2022 The Authors. Angewandte Chemie International Edition published by Wiley-VCH GmbH

15213773, 0, Downloaded from https://onlinelibrary.wiley.com/doi/10.1002/anie.202210828 by National Medical Library The Director, Wiley Online Library on [01/12/2022]. See the Terms and Conditions (https://onlinelibrary.wiley.com/terms-and-conditions) on Wiley Online Library for rules of use; OA articles are governed by the applicable Creative Commons License

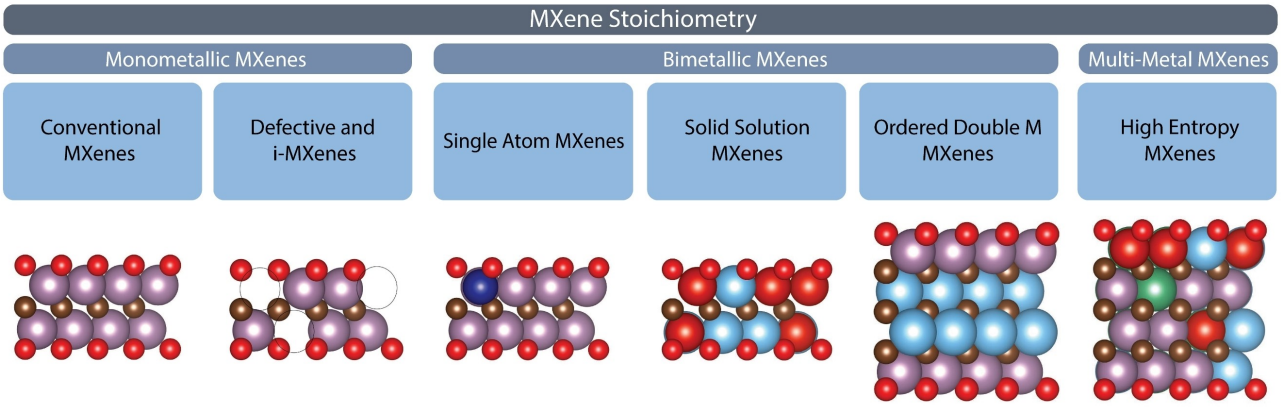

Figure 1. Schematic depicting different MXene stoichiometries, ranging from monometallic MXenes (conventional and *i*-MXenes), bimetallic MXenes (single atom, solid solution and ordered double MXenes), and multi-metallic high entropy MXenes.

MXene, the Mo_2C was delaminated, increasing the number of exposed sites on the active basal plane. In various theoretical studies single-metal MXenes have also shown significant promise in the nitrogen reduction reaction (NRR).[28,29] For instance, it was demonstrated that Ti-edge sites and hydroxy surface groups act as active sites for NRR, and as such, Ti_3C_2OH quantum dots which have an abundance of edge active sites, demonstrated a high Faradaic efficiency of 13.3 % toward NH_3 at −0.50 V vs. the reversible hydrogen electrode (RHE).[30] Such reports demonstrate that, even for the most commonly used pristine MXene structures, a reasonable electrocatalytic activity can be obtained compared to other established materials such as metal oxides and (oxy)hydroxides. The well-defined and easily tunable MXene structure therefore presents a platform to precisely study the fundamentals of electrocatalytic energy conversion reactions.

2.1.2. *Defective and* i-*MXenes*

Controlled defect formation facilitated by atomic vacancies also presents a promising route to tuning the stoichiometric properties of MXenes, and at this stage this is typically associated with monometallic MXene compositions. The discovery of quaternary in-plane ordered MAX phases (*i*-MAX), which exhibit an ordered atomic structure has resulted in the synthesis of "*i*-MXenes" whereby the selective etching of the secondary and ternary metal component facilitates the formation of ordered defects within the MXene structure. For example, the synthesis of $Mo_{1.33}C$ MXenes with divacancy ordering has been reported through the etching of $(Mo_{2/3}Sc_{1/3})_2AlC$.[31] $Nb_{1.33}C$ has also been synthesized from a $(Nb_{2/3}Sc_{1/3})_2AlC$ MAX phase, however in this material, the vacancies were not ordered forming a random distribution.[32] The specific design of the MAX phase to allow for the removal of a sacrificial M-site was also shown to facilitate the synthesis of MXenes with constituent elements which could otherwise not be synthesized. Thus, research which focusses on the incorporation of unconventional M-sites within the MXene structure could benefit significantly by using the *i*-MXene configuration. For example, while the instability of W_2AlC prevents the synthesis of $W_{1.33}CT_x$, using an *i*-MAX phase consisting of $(W_{2/3}Sc_{1/3})_2AlC$ circumvents such issues and allows for the formation of W-based MXenes ($W_{1.33}C$).[33] This proves to be particularly significant as the W_2C MXene was theoretically predicted to exhibit excellent catalytic performance towards HER under high surface H-adsorption.[34]

More broadly, the existence of defects can also improve the electrocatalytic performance of MXenes compared to their pristine counterparts, and it is hypothesized that hydrogen bound in certain vacancy sites has adsorption energies that are favourable for HER.[35] The role of atomic vacancies (associated with M and X atoms) in tuning the band structure of the MXene and subsequently altering the free energy of intermediates associated with the CO_2 reduction reaction (CO_2RR) was investigated.[36] While M vacancies typically strengthen the bond with fragment-type intermediates (such as *COOH and *CHO), X vacancies were shown to weaken this bond. This is unlike alternating molecular-type intermediates (such as *HCOOH and $*H_2CO$) which are not significantly effected by vacancies as they are bound to the MXene surface with weaker van der Waals forces. Overall, this allows for the rational design of defective MXenes which reduce the overall limiting potential for CO_2RR and possibly allows for the tuning of product selectivity. These promising findings warrant further studies to uncover structure-property-function relationships amongst defective MXenes.

2.2. *Bimetallic MXenes*

2.2.1. *Single Atom Modification*

Incorporation of transition metal single sites, specifically Co, in the Mo_2CT_x MXene leads to the tuning of the *H binding energy of multiple sites within the MXene structure, implying that the inclusion of additional elements into the

© 2022 The Authors. Angewandte Chemie International Edition published by Wiley-VCH GmbH

15213773, 0, Downloaded from https://onlinelibrary.wiley.com/doi/10.1002/anie.202210828 by National Medical Library The Director, Wiley Online Library on [01/12/2022]. See the Terms and Conditions (https://onlinelibrary.wiley.com/terms-and-conditions) on Wiley Online Library for rules of use; OA articles are governed by the applicable Creative Commons License

MXene matrix might not only change the electronic properties of that specific site, but rather a range of neighbouring sites within the MXene framework.[37] Indeed, Co-substituted Mo_2CT_x was the first demonstration of a MXene covalently substituted with a middle to late transition metal, significantly improving its HER performance. This work proves significant in the development of MXene electrocatalysts as the incorporation of an additional chemistry which is not typically associated with MXene compositions allows for tuning of bulk chemical and electronic properties of MXenes, and increases the compositional space of MXenes significantly. To synthesize Mo_2CT_x:Co, a standard etching and delamination procedure was used on a bulk bimetallic carbide β-Mo_2C:Co precursor. In this work, the Co single atom sites were shown to be covalently bonded in the Mo_2CT_x MXene, substituting Mo. In addition to the example above, a plethora of other works related to electrocatalysis have exploited the benefits associated with the incorporation of single atom sites. For instance, the ability of $Ti_3C_2T_x$ to act as a host for Ru single atoms was demonstrated, forming a highly efficient HER electrocatalyst.[16] By using a freeze drying method to absorb Ru cations and incorporate thiourea and subsequent annealing to dope N, S and Ru into the structure, the catalyst Ru_{SA}-N-S-$Ti_3C_2T_x$ was obtained. This work suggests that the Ru single atoms act as active sites, and the interaction with the MXene induces a charge transfer that leads to non-bonding states around the Fermi level. In this example, the Ru single atoms were shown to be coordinated to N and S atoms. Overall, incorporation of Ru leads to the weakening of *H adsorption, improving HER performance compared to N-S-$Ti_3C_2T_x$. Another notable example has been demonstrated whereby the strong covalent interactions between Pt single atoms and a vacancy rich $Mo_2TiC_2T_x$ support also led to outstanding HER performance.[14] Using an electrochemical exfoliation method to create Mo vacancies, single Pt atoms were incorporated into the MXene structure forming $Mo_2TiC_2T_x$-Pt_{SA}. The immobilization of Pt in Mo vacancies resulted in the formation of Pt–C and Pt–O bonds.

The above works demonstrate the range of methods and mechanisms in which single atoms can be incorporated into the MXene structure, guiding future research in which MXenes with single atom substituents can be rationally designed to tune intermediate adsorption energies, leading to efficient electrocatalysis potentially beyond HER. To demonstrate the potential application of single atom modified MXenes in catalyzing reactions other than HER, we have performed DFT calculations for a series of structures consisting of $Mo_2C(O_x)(OH)_{2-x}$ with Fe-substitution (i.e. $Mo_2C(O_x)(OH)_{2-x}$:Fe) to investigate their ability to catalyze NRR (iron was selected as the substituent to mimic the composition of the active site of FeMo nitrogenase[38]). Firstly, to account for effects of surface coverage in these systems, our calculations indicated that the average energy of the protonation of O-terminations for the Fe-substituted material (i.e. reaction Mo_2CO_2:Fe + H_2 = → $Mo_2C(OH)_2$:Fe) is 0.73 eV (0.83 eV for unsubstituted Mo_2CO_2), which does not exceed the potential of the NRR rate-limiting step (see below), thus justifying the use of a OH covered surface for modelling the NRR energy profile. Indeed, we found that surface protonation (molybdenum reduction) strongly increases the affinity of both Mo_2CO_2:Fe and 2D-Mo_2CO_2 to N_2, in accordance with experimental results on model molecular Mo-containing complexes.[39,40] Specifically for the fully OH-covered $Mo_2C(OH)_2$:Fe surface (featuring a single coordination vacancy in the vicinity of a Fe site), the adsorption energy of N_2 is ca. 1.2 eV more negative with respect to the O-terminated surface.

We have considered two possible electron–proton transfer pathways, i.e. distal and alternating pathways, as illustrated in Figure 2.[42,43] For both Fe-substituted and unsubstituted molybdenum carbide, $*N_2$ protonation and reduction via the distal pathway was calculated to be more thermodynamically favorable, with the determining step (defined as the most endergonic $1H^+/1e^-$ transfer step) equal to 0.95 eV for $Mo_2C(OH)_2$:Fe and 1.86 eV for $Mo_2C(OH)_2$ implying a substantially higher catalytic activity of Mo_2CT_x:Fe. We have found that generation of the intermediate diazene *NHNH preceding the formation of N_2H_4 via the alternating mechanism requires a comparable energy input (1.02 eV for $Mo_2C(OH)_2$:Fe). Our calculations demonstrate that single site metal substitution in molybdenum carbide can impact strongly its catalytic activity in the NRR by altering the adsorption energies of reaction intermediates. Further experimental work should be undertaken to understand how the competing HER (proceeding with substantially lower theoretical overpotentials than NRR) can be suppressed in such systems, for example, through tuning surface functionalization (see below). Overall, there is strong evidence that the strategy based on single atom substitution in a MXene matrix can be generally applicable for the design of efficient catalysts for a variety of applications and provides an additional degree of freedom in the engineering of active catalysts based on MXenes.

2.2.2. Ordered Double Transition Metal MXenes

The synthesis of ordered double transition metal MXenes has proven to be an effective method allowing for the incorporation of a second metal element into the MXene structure. The ordered incorporation of metal layers into the MXene further extends the range of chemistries contained within the MXene family. Unlike single atom incorporation into the MXene, the high concentration of the secondary metal in this case is so far limited to the inclusion of early transition metals which show great affinity to be incorporated into the MXene structure. However, their ordered nature allows for a well-defined platform which is useful for understanding fundamental structure-property-function relationships in bimetallic MXene electrocatalysts. Anasori and co-workers undertook a comprehensive theoretical study to understand the stability of these bimetallic MXenes.[44] They found that there are at least 26 ordered double metal MXenes, where Mo and Cr typically tend to prefer the outer layers, while Nb and Ta prefer the central layers. Regarding their application to HER, 24 ordered

© 2022 The Authors. Angewandte Chemie International Edition published by Wiley-VCH GmbH

15213773, 0, Downloaded from https://onlinelibrary.wiley.com/doi/10.1002/anie.202210828 by National Medical Library The Director, Wiley Online Library on [01/12/2022]. See the Terms and Conditions (https://onlinelibrary.wiley.com/terms-and-conditions) on Wiley Online Library for rules of use; OA articles are governed by the applicable Creative Commons License

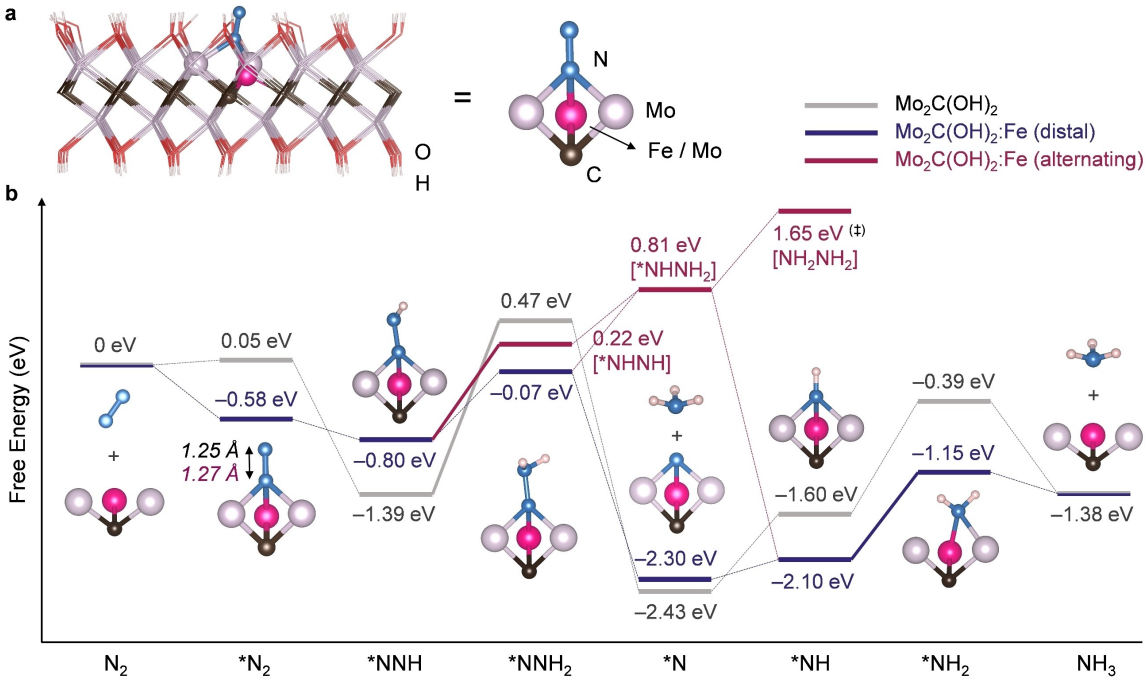

Figure 2. a) Schematic representation of the Mo_2CT_x:Fe structure and [M_3C] core (M = Mo, Fe), where the coordination and hydrogenation/reduction of N_2 takes place. b) DFT-computed free energy diagram for N_2 reduction catalyzed by $Mo_2C(OH)_2$:(Fe), i.e. the reaction $N_2 + 6H^+ + 6e^- = 2NH_3$. Adsorption energies of the reaction products (N_2H_4, NH_3) and species forming prior to the products release (*NNH_3) were found to be close to 0 eV for both $Mo_2C(OH)_2$:Fe and $Mo_2C(OH)_2$ and are not shown in the diagram. Gibbs free energy of formation of gaseous N_2H_4 was taken from an experimental database[41] (designated by "+").

double transition metal MXenes were screened to determine their stability and activity.[45] Out of the materials screened, the lowest Gibbs free energy for *H (ΔG_H) was found on the $Mo_2NbC_2O_2$ surface (0.003 eV), which could indicate that such a composition would possess high HER activity. This study showed that the chemical properties of the basal plane are mainly influenced by the outer transition metal layer, however, it can be tuned by the secondary metal species in sub-layers. These insights are particularly impactful in the field of catalyst design, as it demonstrates the importance of sub-layer configurations which can be controlled within the MXene structure, and should be considered appropriately in future MXene developments. For example, while $Cr_3C_2O_{1.5}(OH)_{0.5}$ has a ΔG_H value of 0.21 eV, incorporation of Nb to form $Cr_2NbC_2O_{1.25}(OH)_{0.75}$ results in a significantly lower ΔG_H value of −0.09 eV, indicating that the Nb layers beneath the Cr–O and Cr–OH terminated surface lead to an improved catalytic performance. Therefore, compositional design strategies achieved through the selection of the primary and secondary metal in ordered double metal MXenes present an attractive strategy for designing novel MXene electrocatalyst formulations.

2.2.3. Solid Solution MXenes

In a similar vein, solid solution MXenes with the ability to incorporate high concentrations of the secondary metal also offer a platform to finely tune the electronic properties of the material through the MXene stoichiometry. For instance, the systematic synthesis of $Ti_{2-y}Nb_yCT_x$, $Ti_{2-y}V_yCT_x$, and $V_{2-y}Nb_yCT_x$; $y = 0.4$, 0.8, 1.2, and 1.6 through HF etching and delamination of the M_2AX phase was demonstrated.[46] These samples exhibited significant changes to the density of states near the Fermi level. For instance, as the proportion of Nb was increased in the $Ti_{2-y}Nb_yC$ MXene structure, the total density of states at the Fermi level increased due to the higher number of valence electrons in Nb compared to Ti. This tunability is particularly important for electrocatalytic systems as the position of the d-band centre and density of states near the Fermi level are known to significantly alter the intermediate binding energies on metal electrocatalysts.[47] Accordingly, there is effectively an unlimited number of non-stoichiometric combinations of MXenes which can be theoretically synthesized which result in tunable electronic properties. Therefore, the design of such systems may rely on high throughput methods such as through the use of machine learning (see below). Moreover, solid solution MXenes have also shown distinct capacitive properties which can be tuned according to their compositions.[48] The promise of solid solution MXenes as highly efficient HER catalysts has also been supported by computational studies.[49]

© 2022 The Authors. Angewandte Chemie International Edition published by Wiley-VCH GmbH

15213773, 0, Downloaded from https://onlinelibrary.wiley.com/doi/10.1002/anie.202210828 by National Medical Library The Director, Wiley Online Library on [01/12/2022]. See the Terms and Conditions (https://onlinelibrary.wiley.com/terms-and-conditions) on Wiley Online Library for rules of use; OA articles are governed by the applicable Creative Commons License

15213773, 0, Downloaded from https://onlinelibrary.wiley.com/doi/10.1002/anie.202210828 by National Medical Library The Director, Wiley Online Library on [01/12/2022]. See the Terms and Conditions (https://onlinelibrary.wiley.com/terms-and-conditions) on Wiley Online Library for rules of use; OA articles are governed by the applicable Creative Commons License

2.3. High Entropy MXenes

While there exists a plethora of established MXene compositions consisting of traditional mono- and bimetallic configurations, recent advances in MXene synthesis show that the number of MXene compositions can be significantly increased. This is an important implication in the design of MXene electrocatalysts, as the composition of the bulk materials can influence surface properties as discussed above. Catalytic surface and subsurface layers typically consisting of five or more elements, without the segregation of distinct metallic phases (intermetallic segregation) are commonly referred to as high entropy alloys (HEAs). Recent studies have justified investigations into HEA electrocatalysts despite their complexities as the electronic contribution of each element to the overall electronic properties of the alloy can be tuned by changing elemental ratios to give rise to desirable binding energies of adsorbates.[50] In principle, a continuous spectrum of binding environments can be attained by tuning the surface properties of HEAs by varying their metal composition.[51] This allows HEAs to potentially unlock novel materials with sites that have optimal binding energies to drive electrocatalytic reactions efficiently. Indeed, the controllable nanoscale synthesis of HEAs is also considered to be a significant opportunity and challenge in the field, as scaling down physical dimensions of materials can result in innate physical and chemical properties not exhibited by the bulk materials.

There has been significant progress in recent years in the development of well-defined HEA nanostructures, however the uniform and controlled synthesis of such materials with minimal phase impurities presents a significant research challenge in advancing the field. Recently, the first report on high entropy MXenes (HE-MXenes) established a protocol to synthesize equimolar, phase pure, high entropy $M_4C_3T_x$ MXenes, $TiVNbMoC_3T_x$ and $TVCrMoC_3T_x$.[18] The work demonstrated that a high entropy phase stabilization effect allowed for the incorporation of four metals into a stable M_4AlC_3 MAX phase with no other carbide or oxide impurities. The high entropy MAX phase was etched subsequently using aqueous HF and delaminated using tetramethylammonium hydroxide to form the HE-MXene phases, with an interlayer distance of 7.81 and 5.44 Å for $TiVNbMoC_3T_x$ and $TVCrMoC_3T_x$, respectively. Using a combination of scanning electron microscopy energy-dispersive X-ray spectroscopy (SEM EDX) and X-ray photoelectron spectroscopy (XPS) depth profiling, it was confirmed that a near equimolar composition of the high entropy MXene could be achieved even after the use of an aqueous HF based etching method to convert the MAX phase into MXenes. Following this study, a five metal HE-MXene with a uniform elemental distribution derived from a bulk $(Ti_{1/5}V_{1/5}Zr_{1/5}Nb_{1/5}Ta_{1/5})_2AlC$ phase was also reported.[52] Extending on this concept, another HE-MXene composition has been more recently reported with the chemical formula $Ti_{1.1}V_{0.7}Cr_xNb_{1.0}Ta_{0.6}C_3T_x$, through the selective etching of Al from the M_4AX_3 parent MAX phase of $Ti_{1.0}V_{0.7}Cr_{0.05}Nb_{1.0}Ta_{1.0}AlC_3$.[53] The HE-MXene in this case exhibited significantly higher volumetric capacitance compared to other non-HE MXene compositions indicating improved charge storage and transfer capabilities.[53,54]

Specific to catalytic reactions, these findings highlight new areas of opportunities in the use of MXenes combined with HEA theory in developing high performing materials. HE-MXenes can harness established benefits associated with HEAs. Due to the large compositional array of elements which can be incorporated into the MXene structure, certain combinations of elements may result in changes to the d-band position or overall band structure which can eventually result in an optimal binding energy between reactants and the catalyst surface, thus selectively promoting the desired catalytic reaction. Furthermore, this creates a route towards the synthesis of materials with chemical reactivities that are not restrained by the base elements in monometallic or bimetallic systems, improving the surface's position on a Sabatier volcano plot for a given reaction.[50] Due to the high entropy stabilization effect which can reduce severe lattice distortions, HE-MXenes may also exhibit an improved stability compared to the traditional MXene compositions, which may be particularly useful in aqueous electrochemical environments which can oxidize the MXene.[54]

Moreover, the field of electrocatalytic HEAs can also benefit from the use of the MXene structural arrangement. As previously mentioned, MXenes have a series of favourable characteristics which make them strong candidates as electrocatalysts for energy conversion reactions, e.g. tuneable surface terminations, high number of exposed surface sides and metallic conductivity. Further to this, regarding (HEA) electrocatalysts, it is important to control and understand parameters related to particle size and morphology, crystallinity, and defects.[55] Since the synthesis of traditional MXenes has been established to control these parameters (for example by varying etching and delamination protocols), it is expected that these principles will also apply to HEA MXenes, solving another significant challenge in the application of HEA electrocatalysts. Regarding the challenges in controlled synthesis of HEAs, HE-MXenes could provide a route to address issues in this area. Particularly, well-defined structures synthesized in large scales with limited intermetallic impurities remain challenging in the realm of HEAs.[50] The synthesis of high entropy MAX phases followed by an appropriate etching and delamination to create single to few-layered MXene flakes provides one solution. Using an appropriate etching and delamination protocol, the phase purity and elemental distribution of the MAX phase can be retained, while scaling down catalyst dimensions to create nanostructured HEAs in 2D morphologies.[18,52]

To show the potential bulk tunability of MXenes in enhancing energy conversion reactions, we performed DFT calculations which compare the reaction energetics of HER using the recently reported HE-MXene $TiVNbMoC_3$ with the V_4C_3 MXene as an example of an established MXene with M_4C_3 stoichiometry, both with O terminations (Figure 3).[18,56,57] To model the $TiVNbMoC_3$ MXene, each of Ti, V, Nb, and Mo were randomly but stoichiometrically distributed within the M_4C_3 structure. As a catalytic

 © 2022 The Authors. Angewandte Chemie International Edition published by Wiley-VCH GmbH

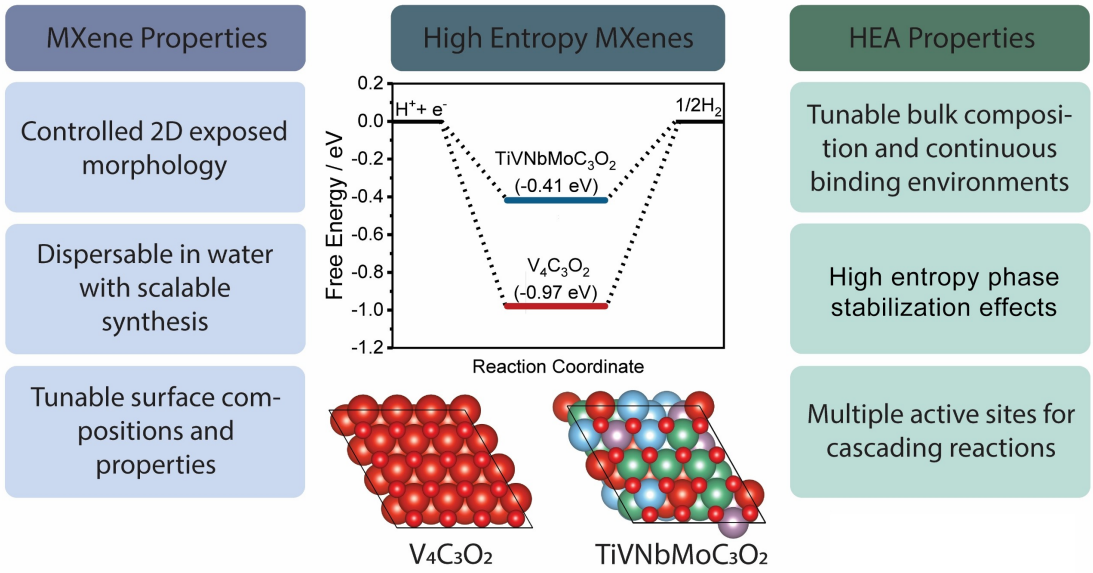

Figure 3. Diagram demonstrating the benefits of MXenes and HEAs which can be harnessed in-tandem when using HE-MXenes. DFT calculated reaction energetics for HER on $TiVNbMoC_3O_2$ and $V_4C_3O_2$ demonstrate that the high entropy configuration resulted in a more favourable band structure for promoting HER.

descriptor, ΔG_H (i.e., free energy of H adsorption) was calculated.[58,59] The results indicate that the HE-MXene displays spontaneous H adsorption, which is much closer to $\Delta G = 0$ eV (−0.41 eV) compared to $V_4C_3O_2$ (−0.97 eV), implying more favourable reaction energetics when using the high entropy configuration. Since the HE-MXene possesses a range of H binding sites on terminal groups (which are connected to a possible combination of T, V, Nb and/or Mo), we also demonstrate that by selecting three random binding sites, the H binding energy could be altered (through the ensemble effect), but was in the range of −0.51 to −0.41 eV (see Supporting Information Table S2). While there is further opportunity to tailor and optimize the bulk chemistry of the MXene in high entropy configurations, these results demonstrate the significance and potential of HE-MXene bulk chemistry in tuning the adsorbate binding strength for HER, potentially extending to a range of other energy conversion reactions.

3. MXene Surface Tuneability

After establishing the tunability of the bulk of MXenes, it is paramount to consider the surface tunability of these systems when considering electrocatalytic reactions. The terminating groups of the material must possess favourable electronic properties, which are influenced by their composition, nature of the outer metal layers and their coordination environment, in addition to the MXene sub-surface structure and composition (consisting of C/N or M components).[60] The surface properties of MXenes are particularly important as it provides the interface at which reaction intermediates transform into products. While there has been significant investigation into MXene stoichiometry, fewer studies have systematically investigated the effect of surface functionalization on electrocatalytic performance. It has been shown that under most synthesis processes, the basal plane of the MXene will be functionalized with terminating groups such as O, OH, F, and Cl.[20]

3.1. Conventional Terminations

Regarding the conventional surface functionalization of MXenes which derive from the wet chemical etching procedures, O, OH, and F terminations on the basal plane are most common. Handoko and co-workers identified that increasing the density of F-terminations on a range of Ti and Mo-based MXenes generally decreased their catalytic performance towards HER, and thus tuned the synthesis conditions to significantly reduce the formation of F-terminations.[10] These simple surface modifications were shown to improve the catalytic performance of Ti and Mo-based MXenes. It was also demonstrated that functional groups play a significant role in the catalytic performance of MXenes toward NRR and CO_2RR. Unlike HER, where F terminations may be detrimental to the catalytic performance, a theoretical study showed that these functional groups may enhance NRR performance due to a decrease in the free energy of the endergonic $*N_2H$ formation step, which can be a rate-limiting step for NRR on MXenes.[29] For CO_2RR, a combined theoretical and experimental study showed that replacing O-terminations with F-terminations on Ti_2CT_x altered the *COOH adsorption energy (making it more endergonic) and thus increasing the magnitude of the theoretical limiting potential. By limiting F-terminations on

© 2022 The Authors. Angewandte Chemie International Edition published by Wiley-VCH GmbH

15213773, 0, Downloaded from https://onlinelibrary.wiley.com/doi/10.1002/anie.202210828 by National Medical Library The Director, Wiley Online Library on [01/12/2022]. See the Terms and Conditions (https://onlinelibrary.wiley.com/terms-and-conditions) on Wiley Online Library for rules of use; OA articles are governed by the applicable Creative Commons License

Ti_2CT_x a Faradaic efficiency of 56% at −1.8 V vs. SHE toward HCOOH production could be attained.[61]

The surfaces of MXenes were even proposed to break scaling relationships in the CO_2RR.[61–63] For example, Handoko et al. showed that on most single-metal O-terminated MXenes the CO_2 reduction pathway to CH_4 prefers the formation of the *HCOOH intermediate due to the O-terminating groups as opposed to the *CO intermediate typically demonstrated on transition metal electrocatalysts.[62] This leads to a minimum energy reaction pathway which is formed by alternating C- and H-bonded intermediates. As such, the C- and H-intermediates follow two different linear scaling relationships (due to the different intermediate coordinating atoms) that can be tuned independently to lower theoretical overpotentials. A similar phenomenon is observed for the production of HCOOH, where both *COOH and *HCOOH intermediates can be stabilized on the terminating group, creating deviations to the linear scaling relationships typically observed on transition metal electrocatalysts.[61] These works demonstrate that even amongst the conventional surface terminations of MXenes, there are significant opportunities to modulate their role in determining overall reaction energetics.

3.2. Unconventional Terminations

To date, no studies have shown the effect of surface terminating groups extending beyond conventional terminations to include NH, S, Br, I, Se, and Te terminations on electrocatalytic energy conversion reactions, although the surface composition of catalysts plays a crucial role in determining a material's catalytic activity. In other 2D materials such as graphene, surface functionalization by electronegative species was shown to lead to a significant alteration of the material's electronic properties.[64,65] As methods to create tuneable surface terminations on MXenes are rapidly evolving, this is expected to offer new opportunities in the development of MXenes with desirable surface properties for electrocatalytic reactions.

For example, the selective surface functionalization of MXenes beyond the traditional terminating groups can be obtained from a molten salt etching method.[19] Using a combination of, for instance, $CdCl_2$ and $CdBr_2$ salts during the etching process, functionalization by Cl and Br can be achieved. Following this, substitution/elimination reactions typically involving Li salts allow for the exchange of surface Cl or Br groups with ligands such as NH, S, Se, and Te. More recently, an alternative halogen etching method has been established whereby the MAX A-layer elements were removed via a halogen mediated dissociation mechanism, producing $Ti_3C_2T_x$ MXenes with homogeneous Br or I terminations.[66] This method allows for tuneable halogen surface functionalization at room temperature, extending the possible MXene surface chemistries.

Regarding these unconventional functional groups, there are minimal works which have investigated their role in electrocatalysis, hence we briefly discuss some related applications in which the tuned surface electronic properties prove to be beneficial. Surface functionalized $Ti_3C_2T_x$ MXenes were modelled using DFT calculations as potential cathodes for lithium–sulfur batteries.[67] Amongst the S, O, N, F, and Cl surface terminations, S terminations demonstrated the highest adsorption energy for most Li_2S_n species which can reduce undesired shuttling effects, while still ensuring metallic conductivity. More relevant to electrochemical systems, the decomposition of Li_2S to form LiS and Li^+ over $Ti_3C_2S_2$ for applications in lithium–sulfur batteries was found to have the lowest energy barrier compared to other functionalized species, demonstrating an enhanced catalytic performance that was linked to the specific functionalization. In the case of Br and I surface terminated $Ti_3C_2T_x$, a reversible redox activity from the oxidation and reduction of Br and I moieties was observed (originating from Br^-/Br^0 and I^-/I^0) through cyclic voltammetry, in contrast to Cl or O/F terminated MXenes which only demonstrated pseudocapacitive behaviour.[68] The Br and I terminated MXenes also demonstrate flat discharge platforms in galvanostatic charge–discharge experiments, in contrast to Cl or O/F terminated systems which did not exhibit charge/discharge platforms. The significant changes of the surface electrochemical properties of such MXenes were attributed to redox active Br and I terminations between the MXene layers which could cycle from negative to near zero valence states, and as such, these redox active terminating groups may also be applied to electrochemical energy conversion reactions.

To demonstrate the potential of using unconventional surface terminations in electrochemical energy conversion reactions, we present DFT calculations which demonstrate the effects of surface functionalization on ΔG_H, which is used as a catalytic descriptor for HER.[58,59] Using the Ti_2CO_2 MXene as a basis, Figure 4a demonstrates that upon substitution of the O terminations with S terminations, the free energy corresponding to the *H intermediate increases from −1.61 eV to 0.43 eV, i.e. significantly closer to zero. While O terminations on Ti_2CO_2 tend to bind H very strongly, S terminations tend to reduce this adsorption strength considerably, tuning the MXene's affinity to the H adsorbate, and dramatically increasing its activity in catalyzing HER. To demonstrate this tunability further, we also undertook calculations taking the Mo_2CO_2 MXene, known for its experimentally confirmed high activity in HER, as a model system.[11,15] While O surface terminations proved to possess favourable free energies for H adsorption for HER (−0.23 eV), adding adjacent Se terminations tend to alter the MXene's affinity to H adsorbates. For instance, when adding 2 adjacent Se terminations (Mo_2CO_2 – 2 Se), the free energy is increased to 0.08 eV, which is at an even more favourable level for HER (i.e., closer to thermoneutrality). Increasing the Se terminations demonstrates a positive correlation with the H adsorption energy, where the free energy of H adsorption for Mo_2CO_2 – 4Se and Mo_2CO_2 – 6Se were 0.36 eV and 0.62 eV, respectively. These results are significant for two reasons. Firstly, they demonstrate that the rational design of the catalyst surface by controlling terminating groups can be used to improve the catalytic performance of MXenes towards HER. However, just as

© 2022 The Authors. Angewandte Chemie International Edition published by Wiley-VCH GmbH

15213773, 0, Downloaded from https://onlinelibrary.wiley.com/doi/10.1002/anie.202210828 by National Medical Library The Director, Wiley Online Library on [01/12/2022]. See the Terms and Conditions (https://onlinelibrary.wiley.com/terms-and-conditions) on Wiley Online Library for rules of use; OA articles are governed by the applicable Creative Commons License

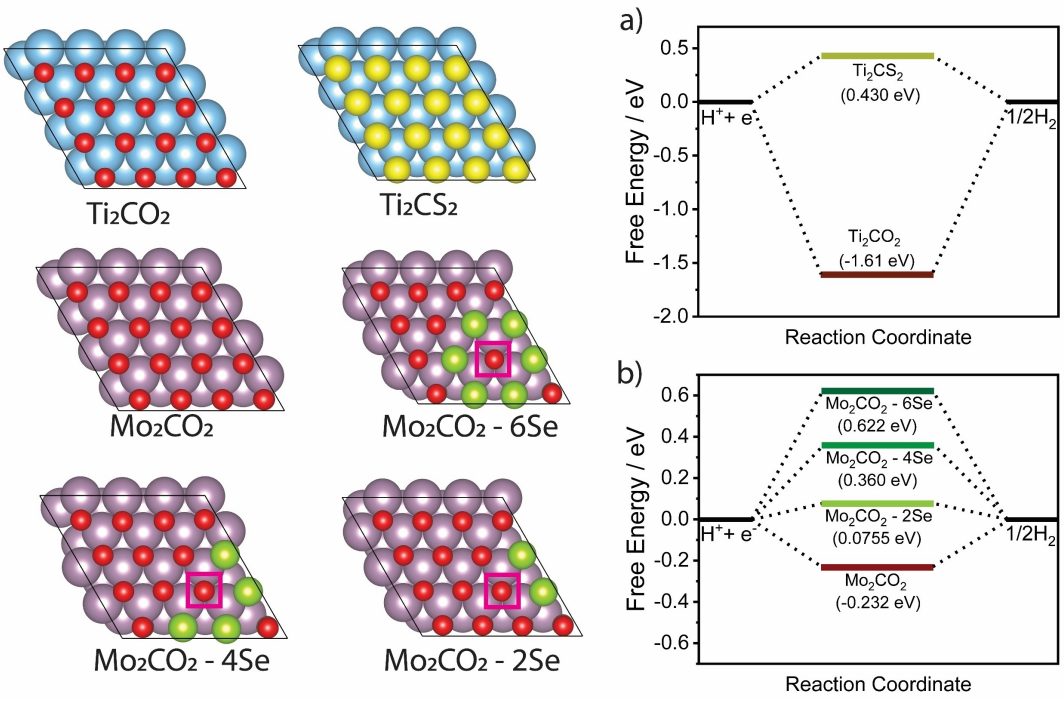

Figure 4. Various MXene structures used to highlight the role of surface terminating groups in altering the affinity of the MXene to H adsorption, a catalytic descriptor of HER (ΔG_H). a) DFT calculated reaction energetics for HER on the Ti_2C MXene with either O or S terminating groups, and b) the Mo_2C MXene with terminating groups consisting of O and Se. For structures in which all hydrogen adsorption sites on functional groups are not equivalent, the pink boxes in the DFT modelled structures indicate the location of H adsorption.

importantly, this aspect of tailoring surface functional groups may also prove to be particularly beneficial when tuning the selectivity away from HER to other energy conversion reactions such as for CO_2RR or nitrogen/nitrate reduction reaction where these cathodic reactions often compete with parasitic HER side reactions.

For instance, one of the first examples of MXene-catalyzed CO_2RR performed by Handoko and co-workers required the use of non-aqueous electrolyte due to the MXene's affinity to hydrogen production from HER.[61] These results warrant further investigation into the synthesis, activity, and stability of unconventional surface terminations in MXenes and their application in energy conversion reactions.

4. MXene Stability During Electrocatalysis

4.1. Challenges in MXene Stability

MXenes are known to be oxidized with relative ease in air or aqueous environments, and as such, it is particularly important to determine the stability of MXenes under electrochemical reaction conditions which have the potential to accelerate the degradation of the MXene.[69,70] While some studies have been undertaken to elucidate the oxidative stability of MXenes as a function of temperature,[71–73] their stability in aqueous environments, under non-neutral pH and under applied potential remains more elusive. Nevertheless, it is known that $Ti_3C_2T_x$ is oxidized to TiO_2 in an aqueous environment according to an exponentially decaying function, and depending on the quality of the precursor chosen, the time constant can be as little as 4–5 days.[74] These results indicate that the decomposition and oxidation of MXenes under catalytically relevant conditions should be considered as this can be potentially detrimental to its application as an electrocatalyst. Furthermore, there is an urgent need to probe the stability of other non-Ti-based MXenes in aqueous environments.[11,37] Computational works have also questioned the stability of MXenes under the conditions of electrocatalytic reactions,[25,75] and therefore both theoretical and experimental studies are required to further understand the dynamic nature of MXenes in conditions relevant to electrocatalysis.

The degradation of MXenes in electrocatalysis presents two significant challenges; firstly, the changes in the MXene chemistry and its physical properties could result in a decrease of the catalytic activity over time, potentially hindering useful applications of the material. Secondly, the decomposition of the MXene could result in the formation of different active sites, which may result in an incorrectly assigned active site in the original MXene, hampering the further development and understanding of MXene electrocatalysts. To verify the stability of MXenes under catalytic reactions, long term stability tests to identify changes in

© 2022 The Authors. Angewandte Chemie International Edition published by Wiley-VCH GmbH

15213773, 0, Downloaded from https://onlinelibrary.wiley.com/doi/10.1002/anie.202210828 by National Medical Library The Director, Wiley Online Library on [01/12/2022]. See the Terms and Conditions (https://onlinelibrary.wiley.com/terms-and-conditions) on Wiley Online Library for rules of use; OA articles are governed by the applicable Creative Commons License

performance, and as importantly, determine chemical and structural changes that occur during the reaction should be undertaken. The in situ and post-mortem characterization will generate insights into the origin of catalytic activity and assess whether the catalytic activity arises from the MXene itself, or its decomposition products. It is important to note that in industrial applications, electrolyzer stacks are commonly expected to last up to 100000 hours in alkaline water electrolyzer systems. Since durability tests in the literature seldom surpass hundreds of hours, it is also important to design accelerated stability tests when considering the design of MXene electrocatalysts for energy conversion reactions.[76]

To this end, we have calculated the phase stability of some commonly used MXenes which are employed in electrocatalytic reactions. While many recent theoretical studies discuss the stability domains of different terminations on MXene surfaces, the bulk (in)stability of MXene materials (particularly under oxidizing conditions, as observed experimentally) is often overlooked, making such calculations rather irrelevant for prediction of the reactivity patterns of actual materials. Our calculations instead estimate the bulk stability regions of selected MXenes to highlight the limits of the applicability of native MXene phases in electrocatalysis.

Figure 5 demonstrates calculated Pourbaix diagrams of Mo_2CO_2 and V_2CO_2 showing the (in)stability of the MXenes, quantified in units of eV/atom, relative to the preferentially formed phase(s). The diagram demonstrates that for both Mo_2CO_2 and V_2CO_2 in multilayer form, the highest thermodynamic stability occurs in the region with high pH and negative potential (green shaded regions in Figure 5). However, in practice, the reduction of the MXene in low pH conditions (for example, during the MAX etching process which can span several days at elevated temperatures) has relatively slow kinetics compared to the rate of A metal removal from the MAX phase. Thus, the Pourbaix diagrams are useful to highlight the importance of the effect of anodic potentials on the overall oxidative stability of the MXene. In addition to this, when considering the oxidation of the MXene, the largest window in which oxidative decomposition may occur is in the alkaline region, where even under negative potential the oxidation of the MXene is still likely, highlighting that caution must be taken when using MXenes in high pH and under anodic potential conditions.

4.2. MXene Stability Under Reaction Conditions

As a representative example of the potential decomposition of MXenes, it was shown that Fe-substituted Mo_2CT_x (Mo_2CT_x:Fe) features a high activity and selectivity towards the 2-electron oxygen reduction reaction (ORR) to generate H_2O_2.[22] However, analysis of the catalyst material unequivocally shows that the MXene Mo_2CT_x:Fe decomposes in O_2-saturated 0.1 M KOH to form a graphitic carbon-like structure with embedded iron oxyhydroxide species, even without an applied bias, confirming the oxidative instability of the MXene in alkaline conditions. The decomposition products of Mo_2CT_x:Fe, rather than the MXene itself, are shown to be the actual catalytically active species. This phenomenon was generalized through experiments on $Ti_3C_2T_x$ and V_2CT_x compositions which demonstrate the complete decomposition of both materials in an O_2-saturated alkaline electrolyte even without applied electric bias. These results confirm the dynamic nature of MXenes under experimental conditions, particularly for alkaline oxygen electrocatalysis. Further to this, it has also been shown that the oxidation of Ti_2CT_x can be accelerated in the presence of H_2O_2,[77] which is a product of the 2-electron ORR reaction pathway.

Overall, considering the high instability of the MXenes in oxidizing environments as followed from theoretical data and experimental results discussed above, the electrocatalytic application of pristine MXene materials (rather than their decomposition products) is limited to the reactions occurring at potentials near the hydrogen evolution or lower (e.g., N_2, CO_2, NO_3^- reduction, etc.), i.e., near or below ca. 0 V vs. the RHE. This highlights a common issue that should be addressed when using MXenes or MXene composites for oxidative reactions. Taking this understanding into consideration, as there have been a range of works involving MXene-based systems in electrocatalysis,[20,78–82] the integrity of the MXene during and after the reaction should be examined to determine the actual catalytically active species, particularly under oxidizing conditions (for example, when catalyzing the oxygen evolution reaction—OER). Careful consideration must be applied when using MXenes for catalytic oxidation reactions to identify the true origin of the catalytic performance which is necessary to further the development of highly active and stable electrocatalysts. It is equally important to consider such stability ranges in computational studies,[83] where it becomes a common practice to disregard the thermodynamic instability of bulk materials when designing the favourable adsorption sites for reaction intermediates.

In addition to chemical stability, physical stability of the MXene should also be considered when designing electrocatalytic systems. Stacking of its 2D nanostructure presents a common issue when using MXenes, which leads to a reduced exposure of active sites and mass/ion transport.[84]

4.3. Stabilization of MXenes

While MXenes are susceptible to transformation under some electrochemical reaction conditions, various strategies typically involving the use of composite structures have been employed to stabilize such systems. To stabilize Mo_2CT_x under electrochemical HER conditions, an in situ sulfurization method was developed which created regions of MoS_2 strongly coupled onto Mo_2CT_x, limiting the further oxidation of the MXene.[85] Without the sulfurized regions, stability tests over 10 days demonstrate the formation of poorly active MoO_3 due to the oxidation of the MXene in the aqueous environment, even at negative potentials. This demonstrates the potential of utilizing composite structures

© 2022 The Authors. Angewandte Chemie International Edition published by Wiley-VCH GmbH

15213773, 0, Downloaded from https://onlinelibrary.wiley.com/doi/10.1002/anie.202210828 by National Medical Library The Director, Wiley Online Library on [01/12/2022]. See the Terms and Conditions (https://onlinelibrary.wiley.com/terms-and-conditions) on Wiley Online Library for rules of use; OA articles are governed by the applicable Creative Commons License

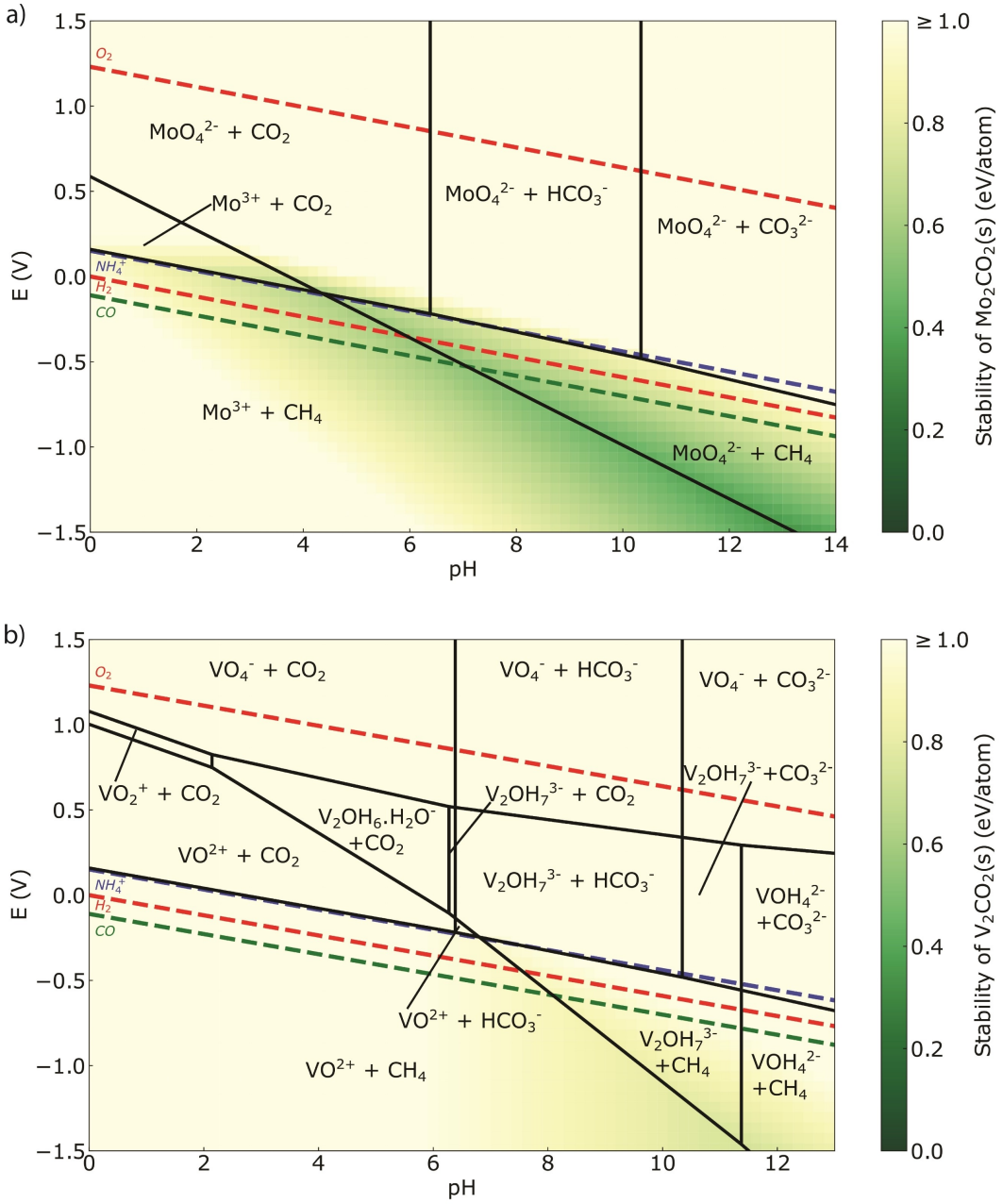

Figure 5. Calculated Pourbaix diagrams of multilayer a) Mo_2CO_2 and b) V_2CO_2 MXenes with a sheet separation of approximately 4 Å. The coloured lines indicate the region of stability of H_2O, CO_2 and N_2 with respect to their reduction and/or oxidation product, representing the conditions required to drive energy conversion reactions (HER/OER, CO_2RR and NRR, respectively). Note: the relative stability of each reaction product for a given pH is not considered (for example, NH_4^+ may be converted into NH_3 in alkaline media).

to enhance MXene stability. Further to this, the formation of MoS_2 was demonstrated to be self-limiting based on the availability of MoO_3 derived from MXene oxidation, and as such its growth did not completely cover the active sites for HER. The use of carbon nanoplating to protect a composite of MoS_2/Ti_3C_2, limiting oxidation of the MXene and promoting long term catalytic stability of the hybrid architecture towards HER in acid, was also demonstrated.[86] However, there are also examples where the formation of hybrid structures did not prevent performance degradation of the material, highlighting the importance of a careful nanoscale design of systems containing multiple components.[78,87,88] Another approach to improving the MXene stability in aqueous environments was developed based on the capping of the edges of MXene flakes in a colloidal dispersion using polyanions, by taking advantage of the positive charge of MXene edges.[89] This method relies on the oxidation mechanism of MXenes whereby the flakes oxidize from the edge inwards.[69,90] To overcome challenges in MXene stacking, various approaches may be used including the formation of composite structures[91] (e.g. rGO/MXene composites) and other 3D architectures[92] (e.g.

© 2022 The Authors. Angewandte Chemie International Edition published by Wiley-VCH GmbH

15213773, 0, Downloaded from https://onlinelibrary.wiley.com/doi/10.1002/anie.202210828 by National Medical Library The Director, Wiley Online Library on [01/12/2022]. See the Terms and Conditions (https://onlinelibrary.wiley.com/terms-and-conditions) on Wiley Online Library for rules of use; OA articles are governed by the applicable Creative Commons License

aerogels and foams), as well as through the use of spacing agents[93,94] (e.g. interlayer spacers or intercalants).

Overall, while MXenes display significant promise in the design of ideal electrocatalysts with promising chemical properties, significant efforts should be invested into improving its stability, as well as selection of appropriate operating conditions. Furthermore, it is crucial to ensure that the reported performance attributed to the MXene is derived from the MXene itself rather than the products of its decomposition.

5. MXene Discovery: Combining DFT and Machine Learning Methods

The announcement of the Materials Genome Initiative in 2011 instigated the advent of a new paradigm for scientific and engineering communities to accelerate materials design, discovery and deployment practices.[95,96] This was made possible via a synergistic amalgamation of experiment, theory and computation in an integrated high throughput fashion. Consequently, a plethora of computational materials databases, such as Materials Project (MP),[97] AFLOWLIB consortium,[98] Open Quantum Materials Database (OQMD),[99] etc., were conceived which complemented traditional and less diverse experimental databases such as the Inorganic Crystal Structure Database (ICSD)[100] and the Crystallographic Open Database (COD).[101] A crucial component of high throughput materials mining workflow is the application of constraints to the database to screen the best candidate according to the desired attribute. The process involves a funnel-like sequence where materials satisfying certain constraints are passed to the subsequent stage while those failing are eliminated, resulting in a subset of materials which outperform the rest in the desired property or any other problem-specific merit—a task ideally suited for machine learning algorithms, tools, and methods.[102] For instance, over 50000 inorganic compounds were screened from the MP database, with stability and band structures as criteria, to discover new potential water splitting photocatalysts.[103] Such data-driven discovery practices urge the push towards a wide scale adaptation of Materials 4.0 by the materials science community.[104]

5.1. Addressing the Large Parameter Space of MXenes

As stipulated in the introduction, MXenes exhibit well-defined 2D structures of the formula $M_{n+1}X_nT_x$, with a wide combination of metals, layering configuration and functional groups. Such exhaustive configurational and compositional space renders MXenes as ideal candidates for high throughput computing and machine learning, especially when high entropy, solid solutions, non-stoichiometric MXenes and surface terminations are also taken into consideration (see schematic in Figure 6).[105] Moreover, there has been a plethora of recent DFT-based studies with different descriptors used for the discovery of promising MXene electrocatalysts.[106–108] This large combinatorial space is particularly relevant for designing MXenes as electrocatalysts since an array of structures and band positioning could ensue tailorable physical and chemical properties to drive favourably a range of energy conversion reactions.

A notable example is the utilization of machine learning models to predict accurately band gaps of functionalized

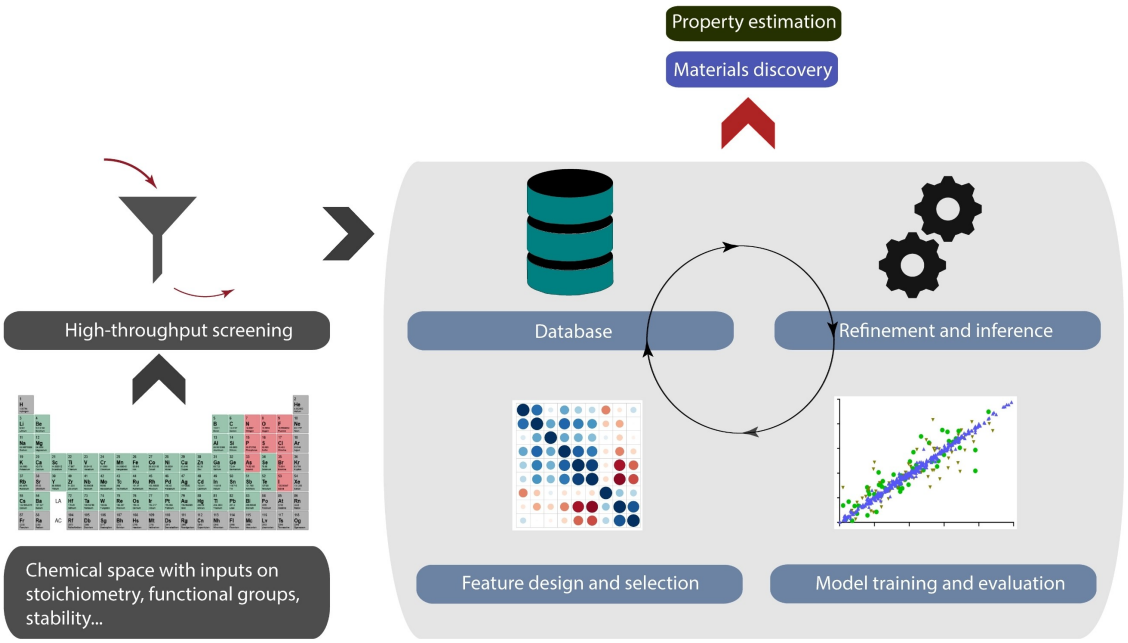

Figure 6. Schematic demonstrating a proposed route to high throughput MXene discovery for application in electrocatalytic energy conversion reactions using machine learning methods.

© 2022 The Authors. Angewandte Chemie International Edition published by Wiley-VCH GmbH

15213773, 0, Downloaded from https://onlinelibrary.wiley.com/doi/10.1002/anie.202210828 by National Medical Library The Director, Wiley Online Library on [01/12/2022]. See the Terms and Conditions (https://onlinelibrary.wiley.com/terms-and-conditions) on Wiley Online Library for rules of use; OA articles are governed by the applicable Creative Commons License

MXenes.[109] Starting from 23870 candidates in the initial database, a finite band gap classification model was used to shortlist 76 candidates based on the band gap range of interest for developing a predictive model with an accuracy of 94%. Feature regularization and reduction via least absolute shrinkage and selection operator (LASSO) reduced the feature set from 47 to 15, which included easily available properties of MXenes such as boiling and melting points, atomic radii of comprising elements, bond lengths (such as mean M/M′-X), etc. Various methods, namely kernel ridge (KRR), support vector (SVR), Gaussian process (GPR), and bootstrap aggregating regression algorithms yielded models which resulted in optimal root mean square error (RMSE) values between 0.14–0.20 eV. It is notable that PBE-level band gaps are often underestimated by DFT, but the model outputs were close to GW-level band gaps which are more accurate but time-consuming to calculate from DFT. This result shows that machine learning can not only provide a quick estimation of band gaps of MXenes but can also bypass band gap underestimation issues associated with local and semi-local DFT functionals without any need for subsequent correction.

When the interest is to use MXenes as electrocatalysts in reactions such as HER, CO_2RR etc., screening of materials is typically dictated by properties related to adsorption behaviour of relevant adsorbates on the active sites and subsequent scaling relationships. For instance, Gibbs free energy of hydrogen adsorption is the fundamental criterion to judge the performance of potential electrocatalysts for HER[59]—a quantity that is challenging and time-consuming to evaluate via DFT calculations. In an attempt to reduce the reliance on DFT and accelerating the screening of hydrogen evolution catalysts for MBenes (transition metal borides; a similar class of 2D materials as MXenes), Sun and co-authors trained machine learning models on 180 MBenes with DFT-calculated adsorption energies.[110] With models such as LASSO, random forest regression (RFR), KRR, and SVR, Co_2B_2 and Mn/Co_2B_2 were discovered as theoretically excellent catalysts for HER. The models also elucidated the underlying factors driving the performance as catalysts, such as ratio of layers, lattice parameters, and metal valence electron number. While these models were applied to the screening of MBenes, these models may also be applied to MXene-based systems.

Another example of machine learning assisting the screening of MXenes reported the identification of activity trends in MXene ordered binary alloys (OBA) with the aim of facilitating the design of these materials as efficient HER electrocatalysts.[111] The authors conducted high throughput DFT calculations based on the Sabatier principle to shortlist 188 types of promising HER catalysts. These calculations indicated that performance of 2D MXene OBAs in HER can be tuned by the alloying effect, albeit intrinsic characteristics governing HER activity were still elusive. The insights were unravelled using machine learning by constructing descriptors for the alloying effect which led to an electronic modification and subsequently constructing an AdaBoost ensemble (a meta-boosting algorithm) learning to predict the HER performance. The selected descriptors were the bond length of oxygen and the surface metal atoms, the distance between the nearest neighbour O atoms, the ionization energy difference, the average affinity energy of the alloy elements, and the number of valence electrons (for X = C or N) which correlated well with the geometrical and electronic factors affected by alloying. With a RMSE of 0.14 eV between the predicted and DFT determined values, the model substantiated that machine learning can reveal the geometric and/or chemical origin of HER activity of MXene OBAs.

5.2. Prospects in Machine Learning for MXenes

Despite these advances, considerable potential still exists in the use of machine learning to support the widespread adoption of MXenes as electrocatalysts. Unlike other 2D counterparts such as graphene, the surface structure of MXenes is fundamentally intricate and dynamic. This complexity in structure arising from factors such as mixed terminal groups, transition metal ordering, high entropy configurations, stoichiometry etc. results in a unique surface chemistry on contact with an electrolyte under bias. Understanding of such structure–activity relationship of MXenes under electrochemical environment is less developed.[105] With deep learning architectures such as crystal graph convolution neural networks, it has become possible to encode intricate structures into machine learning models and map with pertinent information and unravel quantitative structure-activity-property relationships if sufficient data is available.[112] While significant attention is directed towards forward predictive models, for instance predicting the activity of a given structure, considerable value lies in solving the reverse problem, i.e. predicting MXene structures that lead to active, selective, and stable electrocatalysts. A number of techniques, such as generic algorithms, gradient descent, generative adversarial network, etc., are available to optimize complex objective functions and could assist in solving this challenge. Published studies have focused on predicting properties such as band gap and adsorption energy, or estimating HER activity, and highlighting important features governing these predictions. These efforts could continue to formulate machine learning models for other quantities such as *d*-spacing, electric conductivities, and even the role of defects, which are a valuable descriptor for the performance of MXenes, but difficult to measure experimentally and expensive to compute via first-principles. Regardless of exhaustive combinations that may exist in composition space, the volume of data generated for MXenes could potentially bottleneck performance of machine learning protocols. Here, one may explore active learning and Bayesian statistics to systemize model training practices rather than deploying conventional machine learning methods.

© 2022 The Authors. Angewandte Chemie International Edition published by Wiley-VCH GmbH

15213773, 0, Downloaded from https://onlinelibrary.wiley.com/doi/10.1002/anie.202210828 by National Medical Library The Director, Wiley Online Library on [01/12/2022]. See the Terms and Conditions (https://onlinelibrary.wiley.com/terms-and-conditions) on Wiley Online Library for rules of use; OA articles are governed by the applicable Creative Commons License

6. Manufacture of MXene Electrodes

6.1. The Need for Scalable and Tailorable Electrode Synthesis

As electrochemical energy conversion reactions become increasingly technologically feasible and economically viable, large scale catalyst and electrolyzer manufacturing techniques will be required to meet the demand for sustainable chemical and fuel production. Focussing on hydrogen production through electrolysis alone, by 2030, IRENA's planned energy scenario target of deployed electrolyzers is 100 GW.[7] This indicates a dramatic increase in the quantity of electrode materials required. Using proton exchange membrane (PEM) electrolyzers as an example, the 2050 stack size target of 10 MW (operating at 1.7 V and 4 A cm^{-2}) will require approximately 147 m^2 of geometric electrode area. With this consideration in mind, MXene electrocatalysts demonstrate significant promise in industrial application to facilitate energy conversion reactions. It was shown that a 50 time increase in the synthesis scale of $Ti_2C_3T_x$ (from 1 g to 50 g, see Figure 7) could be achieved using large batch synthesis methods, where the synthesis conditions between each scale are directly applicable.[113] Furthermore, the chemical and physical properties of MXenes from large- and small-scale synthesis were identical. With an assumed catalyst loading of 0.25 mg cm^{-2}, 50 g of catalyst could theoretically produce 20 m^2 of electrode area, accounting for a significant proportion of area required for the aforementioned 10 MW electrolyzer system, assuming suitable performance and stability. Indeed, Carbon-Ukraine Ltd. in collaboration with the Materials Research Centre (Ukraine) also offer large scale MXene synthesis, with specially designed etching reactors that can produce 100 g of $Ti_3C_2T_x$ per batch.[114] Furthermore, etching methods which reduce or remove the requirement of HF are being developed rapidly, including in situ HF, molten salt, alkali, and electrochemical etching methods, and are discussed in detail in other works.[115]

Alongside this significant increase in the required geometric catalyst area, there is also a projected increase in demand for a range of minerals related to the current energy transition containing elements such as Co, Ni, Cu etc. which are used in a range of clean energy technologies (such as batteries, fuel cells, solar photovoltaics, wind turbines, etc.).[116] These elements are also of significant relevance to the development of electrocatalytic materials. The expected demand of these elements for clean energy technologies is expected to increase by approximately 70 % by 2030 (from 7094 kt in 2020, to 12 141 kt in 2030).[116] Thus, in addition to upscaling the production of electrocatalysts for the clean energy transition, it is imperative to reduce the required mass loading of catalytic materials (by increasing their intrinsic activity and stability), and to avoid materials which are projected to put significant strain on global supply

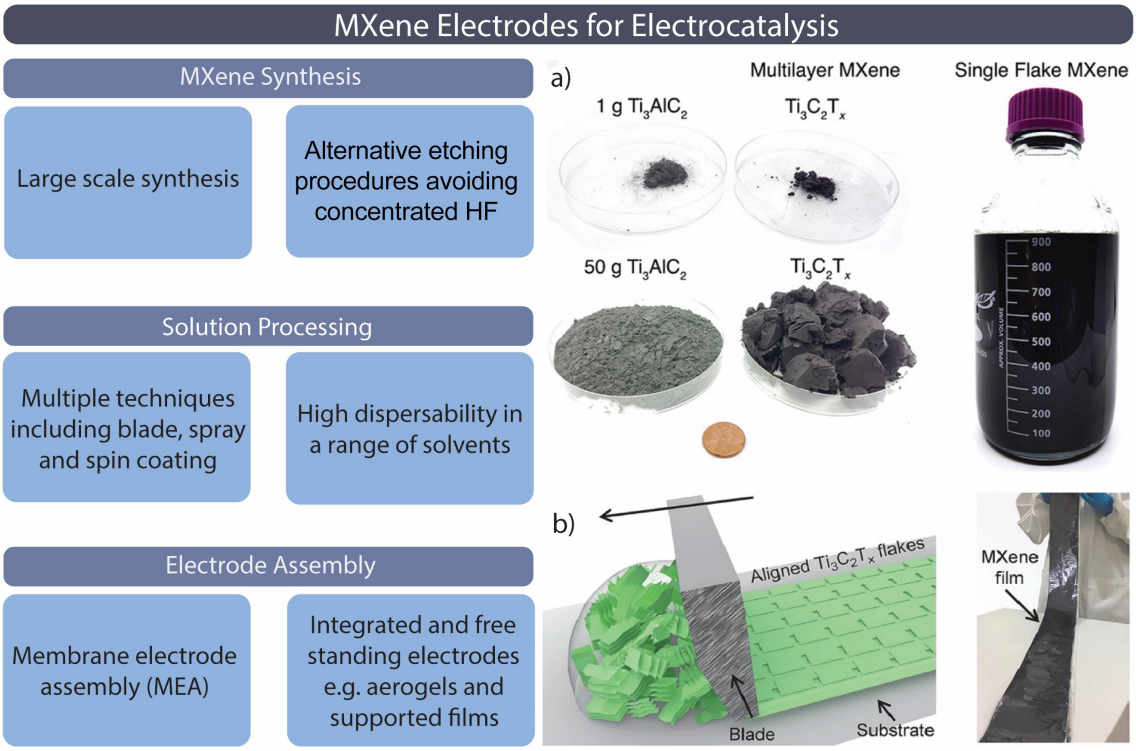

Figure 7. A summary of considerations related to the industrial synthesis of MXene electrodes for electrocatalytic energy conversion reactions. a) Images showing the scaled-up synthesis of $Ti_3C_2T_x$ from 1 g to 50 g (reproduced with permission from ref. [113], © John Wiley & Sons, Inc.). b) Diagram and image showing the large scale synthesis of an aligned MXene film using a blade coating method (reproduced with permission from ref. [122], © John Wiley & Sons, Inc.).

© 2022 The Authors. Angewandte Chemie International Edition published by Wiley-VCH GmbH

15213773, 0, Downloaded from https://onlinelibrary.wiley.com/doi/10.1002/anie.202210828 by National Medical Library The Director, Wiley Online Library on [01/12/2022]. See the Terms and Conditions (https://onlinelibrary.wiley.com/terms-and-conditions) on Wiley Online Library for rules of use; OA articles are governed by the applicable Creative Commons License

chains. The use of precious metals in vast quantities should also be avoided where possible, both due to cost viability and supply chain limitations.[7] As mentioned above, MXenes, due to their tailorable chemical properties, afford the opportunity to have significant improvements in their intrinsic catalytic performance. Furthermore, their 2D morphology leads to high surface areas with an active basal plane, improving exposure of catalytically active sites, allowing for a reduction in the required catalytic material for electrocatalytic applications. In addition to this, the sheer diversity of base materials that can be used to synthesize and/or be incorporated into the MXene also presents an opportunity to avoid the use of cost prohibitive precious metals. This aspect can also allow for the use of materials where abundance and supply chain/life cycle issues can be taken into account.

6.2. Membrane Electrode Assemblies using MXenes

For membrane-based systems where a PEM or anion exchange membrane (AEM) electrolyzer is used, large scale manufacturing techniques to produce the catalyst as well as methods to adhere the catalyst to the membrane to create the membrane electrode assembly (MEA) are required. A range of MEA configurations can be employed revolving around the use of porous transport layers and ionomer coatings depending on the desired properties.[117] For reactions involving a three-phase interface (such as CO_2RR and ORR), these interfaces must be engineered such that the catalyst morphology and wettability can be controlled, allowing for sufficient gaseous mass transport to the active sites.[118] To meet these requirements, controlled high-volume roll-to-roll manufacturing (direct coating of ink onto the membrane, for example, using a slot die for coating on a continuous process) provides a promising opportunity for the large scale manufacturing of catalyst-coated membranes.[119] The high dispersibility and ability to form stable dispersions at varying concentrations give MXenes significant promise in this aspect as well since dispersed inks are required to minimize coating irregularities and defects.

The strong hydrophilicity of MXenes due to polar terminating groups allows them to be soluble in a range of hydrophilic or aqueous solvents such as water, ethanol, dimethyl sulfoxide (DMSO), and *N*,*N*-dimethylformamide (DMF). This will ensure that an appropriate solvent/catalyst combination can be used to create strong adsorptive interactions between the catalyst and different membranes, which make it an attractive precursor in roll-to-roll manufacturing using a range of membrane compositions.[120] The tailorable surface chemistries of the MXene will also prove valuable in this process to create robust binding interactions with the membrane. To ensure that issues surrounding the stacking of MXenes which can limit mass/ion transport are addressed, an ink containing the MXene and a compatible high surface area substrate or interlayer spacer may be used, such as carbon nanotubes, enabling the practical application of MXenes.[94] Further to this, depending on flake size, solvent, and concentration, the viscosity or elasticity of the dispersion can be tuned to create different types of dispersions used for deposition known as inks, slurries, dyes, etc. Importantly, the hydrophilic and conductive properties of MXenes are favourable when used in the catalytic layer, even as a supporting material, as these properties can increase mass and charge transfer to active sites.

6.3. Free-Standing and Integrated Electrode Synthesis

Electrocatalytic energy conversion systems which rely on non-membrane based electrodes (such as the alkaline water electrolyzer) may also require free-standing or integrated electrode systems, whereby there is no requirement to have the catalyst directly coated on a membrane. For these systems, solution processing techniques to generate free-standing structures such as aerogels or films which can be deposited on a variety of substrates (such as current collectors, or other high surface area supports) are essential. Regarding film synthesis, due to the tuneable rheological properties of MXenes, a range of solution processing techniques have been developed which allow for uniform structures to be synthesized on a variety of substrates.[121] For instance, regarding free-standing films, a method to produce large $Ti_3C_2T_x$ films with aligned, high density flakes using a blade coating method was demonstrated.[122] After coating a polypropylene separator membrane, the films could be subsequently peeled off. A free-standing film size of 1×0.1 m was reported in this work, with conductivity up to approximately 15100 S and tensile strength up to approximately 570 MPa, depending on film thickness. There have also been a plethora of other methods used to create MXene films, such as vacuum assisted filtration,[123] spray coating,[124] dip coating,[125] and spin coating.[126]

Aerogel structures have also proven to possess favourable characteristics when considering application in electrocatalysis, derived mainly from their free-standing nature, high surface area, and large interconnected porous structure which allows for efficient reactant and product mobility.[127,128] MXenes can also be processed to create an aerogel framework. For instance, it was reported that a method to synthesize Ti_3C_2/rGO aerogel scaffolds could be achieved through the hydrogel iodine reduction of a mixture containing graphene oxide and the MXene.[129] In addition, an alternative direct freeze-casting method to synthesize a MXene aerogel was demonstrated, where the delaminated MXene is initially frozen and then vacuum dried.[130] These solution processing properties of MXenes prove to be extremely useful and present viable opportunities in the context of designing and manufacturing electrode configurations for energy conversion reactions.

7. Conclusion and Outlook

To summarize, due to their remarkable physical properties and a wide diversity of structures, stoichiometries, and surface functionalities, MXenes offer a platform to create highly active and selective electrocatalysts for key energy

© 2022 The Authors. Angewandte Chemie International Edition published by Wiley-VCH GmbH

15213773, 0, Downloaded from https://onlinelibrary.wiley.com/doi/10.1002/anie.202210828 by National Medical Library The Director, Wiley Online Library on [01/12/2022]. See the Terms and Conditions (https://onlinelibrary.wiley.com/terms-and-conditions) on Wiley Online Library for rules of use; OA articles are governed by the applicable Creative Commons License

conversion reactions. Some of the latest advances in MXene development, such as in high entropy and solid solution structures, as well as in unconventional surface functional groups, have yet to be explored in depth in relation to improving their electrocatalytic activity. Our DFT calculations reveal promising prospects in using these advances to improve the electrocatalytic performance of MXenes for energy conversion reactions, for example, through heteroatom incorporation, high entropy compositions, and surface functionality tuning which can improve the MXene's performance in NRR, HER, and tune the MXene's affinity to H. Furthermore, our Review emphasizes the importance of considering the stability of MXenes under electrochemical conditions by presenting Pourbaix diagrams highlighting the caution that must be taken when using the MXene under anodic potentials and high pH. Due to this, to advance the development of MXene electrocatalysts, the MXene stability under operando conditions must be considered to identify and characterize the true active site, which may change over time. We also present the benefits of combining machine learning and DFT calculations in addressing the large parameter space in MXene discovery. Due to the structural complexities associated with MXenes, particularly when considering changes that arise under operando conditions, we postulate that deep learning architectures such as crystal graph convolutional neural networks may prove to be beneficial when designing machine learning models to screen and identify promising MXene electrocatalysts. Furthermore, these endeavours may be advanced through the use of active learning and Bayesian statistics which can systemize model training practices, addressing the large parameter space and volume of data associated with such models. Finally, we provide insights into the large scale synthesis and wide array of solution processing techniques which is important for the potential industrial application of MXene electrocatalysts. The large scale synthesis of MXenes has been shown through etching protocols that can generate up to 100 g of MXenes per batch presenting promise for future industrial scale synthesis. Furthermore, the range of solution processing techniques such as vacuum assisted filtration, spray, dip and spin coating, and the versatile dispersibility of MXenes allow for the construction of a variety of MEA and free-standing electrodes, which may eventually be used to incorporate MXenes into electrolyzer systems. Overall, further advancement in these four main topics, that is, MXene discovery, performance, stability and large-scale synthesis, will unlock the potential of MXenes in the clean energy transition.

Acknowledgements

We kindly thank Dr. Christopher E. Shuck and Prof. Yury Gogotsi for the fruitful discussions related to topics in this Review. This publication was created as part of NCCR Catalysis (grant number 180544), a National Centre of Competence in Research funded by the Swiss National Science Foundation. We also acknowledge funding from the Swiss National Science Foundation under grant number 196943. Financial support was also provided by the Australian Research Council (ARC) Training Centre for The Global Hydrogen Economy (IC200100023). C.T. was supported by funding provided by the Swiss Federal Commission for Scholarships for Foreign Students. Open Access publishing facilitated by University of New South Wales, as part of the Wiley - University of New South Wales agreement via the Council of Australian University Librarians.

Conflict of Interest

The authors declare no conflict of interest.

Keywords: Density Functional Theory · Electrocatalysis · MXene · Pourbaix Diagram · Stability

[1] N. S. Lewis, D. G. Nocera, *Proc. Natl. Acad. Sci. USA* **2006**, *103*, 15729.
[2] S. Chu, A. Majumdar, *Nature* **2012**, *488*, 294–303.
[3] R. Daiyan, I. MacGill, R. Amal, *ACS Energy Lett.* **2020**, *5*, 3843–3847.
[4] J. Kibsgaard, I. Chorkendorff, *Nat. Energy* **2019**, *4*, 430–433.
[5] P. De Luna, C. Hahn, D. Higgins, S. A. Jaffer, T. F. Jaramillo, E. H. Sargent, *Science* **2019**, *364*, eaav3506.
[6] Z. W. Seh, J. Kibsgaard, C. F. Dickens, I. Chorkendorff, J. K. Nørskov, T. F. Jaramillo, *Science* **2017**, *355*, eaad4998.
[7] E. Taibi, H. Blanco, R. Miranda, M. Carmo, *Green Hydrogen Cost Reduction: Scaling up Electrolysers to Meet the 1.5°C Climate Goal*, IRENA, Abu Dhabi, **2020**.
[8] M. Naguib, M. Kurtoglu, V. Presser, J. Lu, J. Niu, M. Heon, L. Hultman, Y. Gogotsi, M. W. Barsoum, *Adv. Mater.* **2011**, *23*, 4248–4253.
[9] Y. Gogotsi, B. Anasori, *ACS Nano* **2019**, *13*, 8491–8494.
[10] A. D. Handoko, K. D. Fredrickson, B. Anasori, K. W. Convey, L. R. Johnson, Y. Gogotsi, A. Vojvodic, Z. W. Seh, *ACS Appl. Energy Mater.* **2018**, *1*, 173–180.
[11] Z. W. Seh, K. D. Fredrickson, B. Anasori, J. Kibsgaard, A. L. Strickler, M. R. Lukatskaya, Y. Gogotsi, T. F. Jaramillo, A. Vojvodic, *ACS Energy Lett.* **2016**, *1*, 589–594.
[12] T. F. Jaramillo, K. P. Jorgensen, J. Bonde, J. H. Nielsen, S. Horch, I. Chorkendorff, *Science* **2007**, *317*, 100–102.
[13] A. VahidMohammadi, J. Rosen, Y. Gogotsi, *Science* **2021**, *372*, eabf1581.
[14] J. Zhang, Y. Zhao, X. Guo, C. Chen, C.-L. Dong, R.-S. Liu, C.-P. Han, Y. Li, Y. Gogotsi, G. Wang, *Nat. Catal.* **2018**, *1*, 985–992.
[15] S. Intikhab, V. Natu, J. Li, Y. Li, Q. Tao, J. Rosen, M. W. Barsoum, J. Snyder, *J. Catal.* **2019**, *371*, 325–332.
[16] V. Ramalingam, P. Varadhan, H.-C. Fu, H. Kim, D. Zhang, S. Chen, L. Song, D. Ma, Y. Wang, H. N. Alshareef, J.-H. He, *Adv. Mater.* **2019**, *31*, 1903841.
[17] C. Ling, L. Shi, Y. Ouyang, J. Wang, *Chem. Mater.* **2016**, *28*, 9026–9032.
[18] S. K. Nemani, B. Zhang, B. C. Wyatt, Z. D. Hood, S. Manna, R. Khaledialidusti, W. Hong, M. G. Sternberg, S. K. R. S. Sankaranarayanan, B. Anasori, *ACS Nano* **2021**, *15*, 12815–12825.
[19] V. Kamysbayev, A. S. Filatov, H. Hu, X. Rui, F. Lagunas, D. Wang, R. F. Klie, D. V. Talapin, *Science* **2020**, *369*, 979–983.
[20] Y. Wang, Y. Nian, A. N. Biswas, W. Li, Y. Han, J. G. Chen, *Adv. Energy Mater.* **2021**, *11*, 2002967.
[21] A. Bhat, S. Anwer, K. S. Bhat, M. I. H. Mohideen, K. Liao, A. Qurashi, *NPJ 2D Mater. Appl.* **2021**, *5*, 61.

© 2022 The Authors. Angewandte Chemie International Edition published by Wiley-VCH GmbH

15213773, 0, Downloaded from https://onlinelibrary.wiley.com/doi/10.1002/anie.202210828 by National Medical Library The Director, Wiley Online Library on [01/12/2022]. See the Terms and Conditions (https://onlinelibrary.wiley.com/terms-and-conditions) on Wiley Online Library for rules of use; OA articles are governed by the applicable Creative Commons License

[22] D. A. Kuznetsov, Z. Chen, P. M. Abdala, O. v Safonova, A. Fedorov, C. R. Müller, *J. Am. Chem. Soc.* **2021**, *143*, 5771–5778.
[23] R. Ibragimova, M. J. Puska, H.-P. Komsa, *ACS Nano* **2019**, *13*, 9171–9181.
[24] M. Ashton, K. Mathew, R. G. Hennig, S. B. Sinnott, *J. Phys. Chem. C* **2016**, *120*, 3550–3556.
[25] M. Ashton, N. Trometer, K. Mathew, J. Suntivich, C. Freysoldt, S. B. Sinnott, R. G. Hennig, *J. Phys. Chem. C* **2019**, *123*, 3180–3187.
[26] P. Sabatier, *Ber. Dtsch. Chem. Ges.* **1911**, *44*, 1984–2001.
[27] T. Bligaard, J. K. Nørskov, S. Dahl, J. Matthiesen, C. H. Christensen, J. Sehested, *J. Catal.* **2004**, *224*, 206–217.
[28] L. M. Azofra, N. Li, D. R. MacFarlane, C. Sun, *Energy Environ. Sci.* **2016**, *9*, 2545–2549.
[29] L. R. Johnson, S. Sridhar, L. Zhang, K. D. Fredrickson, A. S. Raman, J. Jang, C. Leach, A. Padmanabhan, C. C. Price, N. C. Frey, A. Raizada, V. Rajaraman, S. A. Saiprasad, X. Tang, A. Vojvodic, *ACS Catal.* **2020**, *10*, 253–264.
[30] Z. Jin, C. Liu, Z. Liu, J. Han, Y. Fang, Y. Han, Y. Niu, Y. Wu, C. Sun, Y. Xu, *Adv. Energy Mater.* **2020**, *10*, 2000797.
[31] Q. Tao, M. Dahlqvist, J. Lu, S. Kota, R. Meshkian, J. Halim, J. Palisaitis, L. Hultman, M. W. Barsoum, P. O. Å Persson, J. Rosen, *Nat. Commun.* **2017**, *8*, 14949.
[32] J. Halim, J. Palisaitis, J. Lu, J. Thörnberg, E. J. Moon, M. Precner, P. Eklund, P. O. Å Persson, M. W. Barsoum, J. Rosen, *ACS Appl. Nano Mater.* **2018**, *1*, 2455–2460.
[33] R. Meshkian, M. Dahlqvist, J. Lu, B. Wickman, J. Halim, J. Thörnberg, Q. Tao, S. Li, S. Intikhab, J. Snyder, M. W. Barsoum, M. Yildizhan, J. Palisaitis, L. Hultman, P. O. Å Persson, J. Rosen, *Adv. Mater.* **2018**, *30*, 1706409.
[34] H. Pan, *Sci. Rep.* **2016**, *6*, 32531.
[35] H. Lind, B. Wickman, J. Halim, G. Montserrat-Sisó, A. Hellman, J. Rosen, *Adv. Sustainable Syst.* **2021**, *5*, 2000158.
[36] H. Chen, A. D. Handoko, T. Wang, J. Qu, J. Xiao, X. Liu, D. Legut, Z. Wei Seh, Q. Zhang, *ChemSusChem* **2020**, *13*, 5690–5698.
[37] D. A. Kuznetsov, Z. Chen, P. v Kumar, A. Tsoukalou, A. Kierzkowska, P. M. Abdala, O. v Safonova, A. Fedorov, C. R. Müller, *J. Am. Chem. Soc.* **2019**, *141*, 17809–17816.
[38] T. Spatzal, M. Aksoyoglu, L. Zhang, S. L. A. Andrade, E. Schleicher, S. Weber, D. C. Rees, O. Einsle, *Science* **2011**, *334*, 940.
[39] D. V. Yandulov, R. R. Schrock, *Science* **2003**, *301*, 76–78.
[40] T. A. Bazhenova, A. E. Shilov, *Coord. Chem. Rev.* **1995**, *144*, 69–145.
[41] D. R. Lide, *CRC Handbook of Chemistry and Physics*, CRC Press, Boca Raton, **2005**.
[42] F. Neese, *Angew. Chem. Int. Ed.* **2006**, *45*, 196–199; *Angew. Chem.* **2006**, *118*, 202–205.
[43] B. M. Hoffman, D. Lukoyanov, Z.-Y. Yang, D. R. Dean, L. C. Seefeldt, *Chem. Rev.* **2014**, *114*, 4041–4062.
[44] B. Anasori, Y. Xie, M. Beidaghi, J. Lu, B. C. Hosler, L. Hultman, P. R. C. Kent, Y. Gogotsi, M. W. Barsoum, *ACS Nano* **2015**, *9*, 9507–9516.
[45] D. Jin, L. R. Johnson, A. S. Raman, X. Ming, Y. Gao, F. Du, Y. Wei, G. Chen, A. Vojvodic, Y. Gogotsi, X. Meng, *J. Phys. Chem. C* **2020**, *124*, 10584–10592.
[46] M. Han, K. Maleski, C. E. Shuck, Y. Yang, J. T. Glazar, A. C. Foucher, K. Hantanasirisakul, A. Sarycheva, N. C. Frey, S. J. May, V. B. Shenoy, E. A. Stach, Y. Gogotsi, *J. Am. Chem. Soc.* **2020**, *142*, 19110–19118.
[47] J. K. Nørskov, F. Abild-Pedersen, F. Studt, T. Bligaard, *Proc. Natl. Acad. Sci. USA* **2011**, *108*, 937–943.
[48] L. Wang, M. Han, C. E. Shuck, X. Wang, Y. Gogotsi, *Nano Energy* **2021**, *88*, 106308.
[49] X. Yang, N. Gao, S. Zhou, J. Zhao, *Phys. Chem. Chem. Phys.* **2018**, *20*, 19390–19397.
[50] T. Löffler, A. Savan, A. Garzón-Manjón, M. Meischein, C. Scheu, A. Ludwig, W. Schuhmann, *ACS Energy Lett.* **2019**, *4*, 1206–1214.
[51] T. A. A. Batchelor, J. K. Pedersen, S. H. Winther, I. E. Castelli, K. W. Jacobsen, J. Rossmeisl, *Joule* **2019**, *3*, 834–845.
[52] Z. Du, C. Wu, Y. Chen, Z. Cao, R. Hu, Y. Zhang, J. Gu, Y. Cui, H. Chen, Y. Shi, J. Shang, B. Li, S. Yang, *Adv. Mater.* **2021**, *33*, 2101473.
[53] J. Zhou, Q. Tao, B. Ahmed, J. Palisaitis, I. Persson, J. Halim, M. W. Barsoum, P. O. Å Persson, J. Rosen, *Chem. Mater.* **2022**, *34*, 2098–2106.
[54] A. S. Etman, J. Zhou, J. Rosen, *Electrochem. Commun.* **2022**, *137*, 107264.
[55] Y. Xin, S. Li, Y. Qian, W. Zhu, H. Yuan, P. Jiang, R. Guo, L. Wang, *ACS Catal.* **2020**, *10*, 11280–11306.
[56] M. H. Tran, T. Schäfer, A. Shahraei, M. Dürrschnabel, L. Molina-Luna, U. I. Kramm, C. S. Birkel, *ACS Appl. Energy Mater.* **2018**, *1*, 3908–3914.
[57] J. Zhou, S. Lin, Y. Huang, P. Tong, B. Zhao, X. Zhu, Y. Sun, *Chem. Eng. J.* **2019**, *373*, 203–212.
[58] J. Greeley, T. F. Jaramillo, J. Bonde, I. Chorkendorff, J. K. Nørskov, *Nat. Mater.* **2006**, *5*, 909–913.
[59] J. K. Nørskov, T. Bligaard, A. Logadottir, J. R. Kitchin, J. G. Chen, S. Pandelov, U. Stimming, *J. Electrochem. Soc.* **2005**, *152*, J23.
[60] Y. Yang, K. Hantanasirisakul, N. C. Frey, B. Anasori, R. J. Green, P. C. Rogge, I. Waluyo, A. Hunt, P. Shafer, E. Arenholz, V. B. Shenoy, Y. Gogotsi, S. J. May, *2D Mater.* **2020**, *7*, 025015.
[61] A. D. Handoko, H. Chen, Y. Lum, Q. Zhang, B. Anasori, Z. W. Seh, *iScience* **2020**, *23*, 101181.
[62] A. D. Handoko, K. H. Khoo, T. L. Tan, H. Jin, Z. W. Seh, *J. Mater. Chem. A* **2018**, *6*, 21885–21890.
[63] Y. Li, Y. Chen, Z. Guo, C. Tang, B. Sa, N. Miao, J. Zhou, Z. Sun, *Chem. Eng. J.* **2022**, *429*, 132171.
[64] M. di Giovannantonio, O. Deniz, J. I. Urgel, R. Widmer, T. Dienel, S. Stolz, C. Sánchez-Sánchez, M. Muntwiler, T. Dumslaff, R. Berger, A. Narita, X. Feng, K. Müllen, P. Ruffieux, R. Fasel, *ACS Nano* **2018**, *12*, 74–81.
[65] F. Karlický, K. Kumara Ramanatha Datta, M. Otyepka, R. Zbořil, *ACS Nano* **2013**, *7*, 6434–6464.
[66] A. Jawaid, A. Hassan, G. Neher, D. Nepal, R. Pachter, W. J. Kennedy, S. Ramakrishnan, R. A. Vaia, *ACS Nano* **2021**, *15*, 2771–2777.
[67] D. Wang, F. Li, R. Lian, J. Xu, D. Kan, Y. Liu, G. Chen, Y. Gogotsi, Y. Wei, *ACS Nano* **2019**, *13*, 11078–11086.
[68] M. Li, X. Li, G. Qin, K. Luo, J. Lu, Y. Li, G. Liang, Z. Huang, J. Zhou, L. Hultman, P. Eklund, P. O. Å Persson, S. Du, Z. Chai, C. Zhi, Q. Huang, *ACS Nano* **2021**, *15*, 1077–1085.
[69] C. J. Zhang, S. Pinilla, N. McEvoy, C. P. Cullen, B. Anasori, E. Long, S.-H. Park, A. Seral-Ascaso, A. Shmeliov, D. Krishnan, C. Morant, X. Liu, G. S. Duesberg, Y. Gogotsi, V. Nicolosi, *Chem. Mater.* **2017**, *29*, 4848–4856.
[70] O. Mashtalir, K. M. Cook, V. N. Mochalin, M. Crowe, M. W. Barsoum, Y. Gogotsi, *J. Mater. Chem. A* **2014**, *2*, 14334–14338.
[71] M. Seredych, C. E. Shuck, D. Pinto, M. Alhabeb, E. Precetti, G. Deysher, B. Anasori, N. Kurra, Y. Gogotsi, *Chem. Mater.* **2019**, *31*, 3324–3332.
[72] Z. Li, L. Wang, D. Sun, Y. Zhang, B. Liu, Q. Hu, A. Zhou, *Mater. Sci. Eng. B* **2015**, *191*, 33–40.
[73] L. Yang, W. Chen, R. Yang, A. Chen, H. Zhang, Y. Sun, Y. Jia, X. Li, Z. Tang, X. Gui, *ACS Appl. Mater. Interfaces* **2020**, *12*, 10755–10762.
[74] C. E. Shuck, M. Han, K. Maleski, K. Hantanasirisakul, S. J. Kim, J. Choi, W. E. B. Reil, Y. Gogotsi, *ACS Appl. Nano Mater.* **2019**, *2*, 3368–3376.

© 2022 The Authors. Angewandte Chemie International Edition published by Wiley-VCH GmbH

15213773, 0, Downloaded from https://onlinelibrary.wiley.com/doi/10.1002/anie.202210828 by National Medical Library The Director, Wiley Online Library on [01/12/2022]. See the Terms and Conditions (https://onlinelibrary.wiley.com/terms-and-conditions) on Wiley Online Library for rules of use; OA articles are governed by the applicable Creative Commons License

[75] B. Wei, Z. Fu, D. Legut, T. C. Germann, S. Du, H. Zhang, J. S. Francisco, R. Zhang, *Adv. Mater.* **2021**, *33*, 2102595.
[76] P. Aßmann, A. S. Gago, P. Gazdzicki, K. A. Friedrich, M. Wark, *Curr. Opin. Electrochem.* **2020**, *21*, 225–233.
[77] B. Ahmed, D. H. Anjum, M. N. Hedhili, Y. Gogotsi, H. N. Alshareef, *Nanoscale* **2016**, *8*, 7580–7587.
[78] M. Yu, S. Zhou, Z. Wang, J. Zhao, J. Qiu, *Nano Energy* **2018**, *44*, 181–190.
[79] J. Wang, P. He, Y. Shen, L. Dai, Z. Li, Y. Wu, C. An, *Nano Res.* **2021**, *14*, 3474–3481.
[80] H. Parse, I. M. Patil, A. S. Swami, B. A. Kakade, *ACS Appl. Nano Mater.* **2021**, *4*, 1094–1103.
[81] M. Yu, J. Zheng, M. Guo, *J. Energy Chem.* **2022**, *70*, 472–479.
[82] D. Guo, X. Li, Y. Jiao, H. Yan, A. Wu, G. Yang, Y. Wang, C. Tian, H. Fu, *Nano Res.* **2022**, *15*, 238–247.
[83] Z. Wang, Y.-R. Zheng, I. Chorkendorff, J. K. Nørskov, *ACS Energy Lett.* **2020**, *5*, 2905–2908.
[84] X. Gao, X. Du, T. S. Mathis, M. Zhang, X. Wang, J. Shui, Y. Gogotsi, M. Xu, *Nat. Commun.* **2020**, *11*, 6160.
[85] K. R. G. Lim, A. D. Handoko, L. R. Johnson, X. Meng, M. Lin, G. S. Subramanian, B. Anasori, Y. Gogotsi, A. Vojvodic, Z. W. Seh, *ACS Nano* **2020**, *14*, 16140–16155.
[86] X. Wu, Z. Wang, M. Yu, L. Xiu, J. Qiu, *Adv. Mater.* **2017**, *29*, 1607017.
[87] Y. Lu, D. Fan, Z. Chen, W. Xiao, C. Cao, X. Yang, *Sci. Bull.* **2020**, *65*, 460–466.
[88] N. C. S. Selvam, J. Lee, G. H. Choi, M. J. Oh, S. Xu, B. Lim, P. J. Yoo, *J. Mater. Chem. A* **2019**, *7*, 27383–27393.
[89] V. Natu, J. L. Hart, M. Sokol, H. Chiang, M. L. Taheri, M. W. Barsoum, *Angew. Chem. Int. Ed.* **2019**, *58*, 12655–12660; *Angew. Chem.* **2019**, *131*, 12785–12790.
[90] A. Lipatov, M. Alhabeb, M. R. Lukatskaya, A. Boson, Y. Gogotsi, A. Sinitskii, *Adv. Electron. Mater.* **2016**, *2*, 1600255.
[91] L. Xiu, Z. Wang, M. Yu, X. Wu, J. Qiu, *ACS Nano* **2018**, *12*, 8017–8028.
[92] Y. Zhu, K. Rajouâ, S. le Vot, O. Fontaine, P. Simon, F. Favier, *Nano Energy* **2020**, *73*, 104734.
[93] J. Tang, X. Huang, T. Qiu, X. Peng, T. Wu, L. Wang, B. Luo, L. Wang, *Chem. Eur. J.* **2021**, *27*, 1921–1940.
[94] M.-Q. Zhao, C. E. Ren, Z. Ling, M. R. Lukatskaya, C. Zhang, K. L. van Aken, M. W. Barsoum, Y. Gogotsi, *Adv. Mater.* **2015**, *27*, 339–345.
[95] The National Science and Technology Council, *Materials Genome Initiative for Global Competitiveness*, Washington D.C., **2011**.
[96] J. J. de Pablo, N. E. Jackson, M. A. Webb, L.-Q. Chen, J. E. Moore, D. Morgan, R. Jacobs, T. Pollock, D. G. Schlom, E. S. Toberer, J. Analytis, I. Dabo, D. M. DeLongchamp, G. A. Fiete, G. M. Grason, G. Hautier, Y. Mo, K. Rajan, E. J. Reed, E. Rodriguez, V. Stevanovic, J. Suntivich, K. Thornton, J.-C. Zhao, *npj Comput. Mater.* **2019**, *5*, 41.
[97] A. Jain, S. P. Ong, G. Hautier, W. Chen, W. D. Richards, S. Dacek, S. Cholia, D. Gunter, D. Skinner, G. Ceder, K. A. Persson, *APL Mater.* **2013**, *1*, 011002.
[98] S. Curtarolo, W. Setyawan, S. Wang, J. Xue, K. Yang, R. H. Taylor, L. J. Nelson, G. L. W. Hart, S. Sanvito, M. Buongiorno-Nardelli, N. Mingo, O. Levy, *Comput. Mater. Sci.* **2012**, *58*, 227–235.
[99] J. E. Saal, S. Kirklin, M. Aykol, B. Meredig, C. Wolverton, *JOM* **2013**, *65*, 1501–1509.
[100] M. Hellenbrandt, *Crystallogr. Rev.* **2004**, *10*, 17–22.
[101] S. Gražulis, D. Chateigner, R. T. Downs, A. F. T. Yokochi, M. Quirós, L. Lutterotti, E. Manakova, J. Butkus, P. Moeck, A. le Bail, *J. Appl. Crystallogr.* **2009**, *42*, 726–729.
[102] G. R. Schleder, A. C. M. Padilha, C. M. Acosta, M. Costa, A. Fazzio, *J. Phys. Mater.* **2019**, *2*, 032001.
[103] X. Zhang, Z. Zhang, D. Wu, X. Zhang, X. Zhao, Z. Zhou, *Small Methods* **2018**, *2*, 1700359.
[104] R. Jose, S. Ramakrishna, *Appl. Mater. Today* **2018**, *10*, 127–132.
[105] C. Zhan, W. Sun, Y. Xie, D. Jiang, P. R. C. Kent, *ACS Appl. Mater. Interfaces* **2019**, *11*, 24885–24905.
[106] T. Hu, M. Wang, C. Guo, C. M. Li, *J. Mater. Chem. A* **2022**, *10*, 8923–8931.
[107] P. Hou, Y. Tian, D. Jin, X. Liu, Y. Xie, F. Du, X. Meng, *J. Phys. D* **2022**, *55*, 464002.
[108] C. Wang, X. Wang, T. Zhang, P. Qian, T. Lookman, Y. Su, *J. Mater. Chem. A* **2022**, *10*, 18195–18205.
[109] A. C. Rajan, A. Mishra, S. Satsangi, R. Vaish, H. Mizuseki, K.-R. Lee, A. K. Singh, *Chem. Mater.* **2018**, *30*, 4031–4038.
[110] X. Sun, J. Zheng, Y. Gao, C. Qiu, Y. Yan, Z. Yao, S. Deng, J. Wang, *Appl. Surf. Sci.* **2020**, *526*, 146522.
[111] X. Wang, C. Wang, S. Ci, Y. Ma, T. Liu, L. Gao, P. Qian, C. Ji, Y. Su, *J. Mater. Chem. A* **2020**, *8*, 23488–23497.
[112] T. Xie, J. C. Grossman, *Phys. Rev. Lett.* **2018**, *120*, 145301.
[113] C. E. Shuck, A. Sarycheva, M. Anayee, A. Levitt, Y. Zhu, S. Uzun, V. Balitskiy, V. Zahorodna, O. Gogotsi, Y. Gogotsi, *Adv. Eng. Mater.* **2020**, *22*, 1901241.
[114] Carbon-Ukraine Ltd., "Etching Reactor for MXene synthesis (acidic etching of MAX-phase powders), productivity up to 100 g per batch," can be found under https://carbon.org.ua/etching-reactor-for-mxene-synthesis, **2022**.
[115] Y. Wei, P. Zhang, R. A. Soomro, Q. Zhu, B. Xu, *Adv. Mater.* **2021**, *33*, 2103148.
[116] IEA, *The Role of Critical Minerals in Clean Energy Transitions*, Paris, **2021**.
[117] M. Bühler, P. Holzapfel, D. McLaughlin, S. Thiele, *J. Electrochem. Soc.* **2019**, *166*, F1070–F1078.
[118] R. Shi, J. Guo, X. Zhang, G. I. N. Waterhouse, Z. Han, Y. Zhao, L. Shang, C. Zhou, L. Jiang, T. Zhang, *Nat. Commun.* **2020**, *11*, 3028.
[119] J. Park, Z. Kang, G. Bender, M. Ulsh, S. A. Mauger, *J. Power Sources* **2020**, *479*, 228819.
[120] K. Maleski, V. N. Mochalin, Y. Gogotsi, *Chem. Mater.* **2017**, *29*, 1632–1640.
[121] B. Akuzum, K. Maleski, B. Anasori, P. Lelyukh, N. J. Alvarez, E. C. Kumbur, Y. Gogotsi, *ACS Nano* **2018**, *12*, 2685–2694.
[122] J. Zhang, N. Kong, S. Uzun, A. Levitt, S. Seyedin, P. A. Lynch, S. Qin, M. Han, W. Yang, J. Liu, X. Wang, Y. Gogotsi, J. M. Razal, *Adv. Mater.* **2020**, *32*, 2001093.
[123] Z. Ling, C. E. Ren, M.-Q. Zhao, J. Yang, J. M. Giammarco, J. Qiu, M. W. Barsoum, Y. Gogotsi, *Proc. Natl. Acad. Sci. USA* **2014**, *111*, 16676.
[124] K. Hantanasirisakul, M.-Q. Zhao, P. Urbankowski, J. Halim, B. Anasori, S. Kota, C. E. Ren, M. W. Barsoum, Y. Gogotsi, *Adv. Electron. Mater.* **2016**, *2*, 1600050.
[125] P. Salles, D. Pinto, K. Hantanasirisakul, K. Maleski, C. E. Shuck, Y. Gogotsi, *Adv. Funct. Mater.* **2019**, *29*, 1809223.
[126] G. Ying, A. D. Dillon, A. T. Fafarman, M. W. Barsoum, *Mater. Res. Lett.* **2017**, *5*, 391–398.
[127] G. Fu, X. Yan, Y. Chen, L. Xu, D. Sun, J.-M. Lee, Y. Tang, *Adv. Mater.* **2018**, *30*, 1704609.
[128] B. Cai, A. Eychmüller, *Adv. Mater.* **2019**, *31*, 1804881.
[129] X. Zhang, R. Lv, A. Wang, W. Guo, X. Liu, J. Luo, *Angew. Chem. Int. Ed.* **2018**, *57*, 15028–15033; *Angew. Chem.* **2018**, *130*, 15248–15253.
[130] R. Bian, G. He, W. Zhi, S. Xiang, T. Wang, D. Cai, *J. Mater. Chem. C* **2019**, *7*, 474–478.

Manuscript received: July 22, 2022
Accepted manuscript online: October 24, 2022
Version of record online: ■■, ■■

© 2022 The Authors. Angewandte Chemie International Edition published by Wiley-VCH GmbH

15213773, 0, Downloaded from https://onlinelibrary.wiley.com/doi/10.1002/anie.202210828 by National Medical Library The Director, Wiley Online Library on [01/12/2022]. See the Terms and Conditions (https://onlinelibrary.wiley.com/terms-and-conditions) on Wiley Online Library for rules of use; OA articles are governed by the applicable Creative Commons License

Reviews

MXene Electrocatalysts

C. Tsounis,* P. V. Kumar, H. Masood, R. P. Kulkarni, G. S. Gautam, C. R. Müller, R. Amal, D. A. Kuznetso* **e202210828**

Advancing MXene Electrocatalysts for Energy Conversion Reactions: Surface, Stoichiometry, and Stability

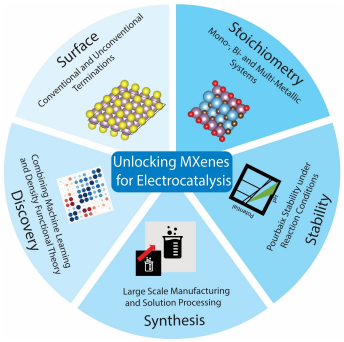

Due to their remarkable physical properties and diversity of chemical structures, MXenes offer a platform to create highly active and selective electrocatalysts for key energy conversion reactions. This Review discusses the latest literature relevant to their application in electrocatalysis and provides a perspective supplemented by new DFT calculations on how MXenes may play a key role in the global sustainable energy transition.

© 2022 The Authors. Angewandte Chemie International Edition published by Wiley-VCH GmbH

15213773, 0, Downloaded from https://onlinelibrary.wiley.com/doi/10.1002/anie.202210828 by National Medical Library The Director, Wiley Online Library on [01/12/2022]. See the Terms and Conditions (https://onlinelibrary.wiley.com/terms-and-conditions) on Wiley Online Library for rules of use; OA articles are governed by the applicable Creative Commons License